CIRP Annals - Manufacturing Technology 69 (2020) 717–739

Contents lists available at ScienceDirect

CIRP Annals - Manufacturing Technology

journal homepage: https://www.editorialmanager.com/CIRP/default.aspx

Manufacturing of multiscale structured surfaces

Ekkard Brinksmeier (1)[a,b], Bernhard Karpuschewski (1)[a,b,*], Jiwang Yan (2)[c], Lars Schönemann[a,b]

[a] Leibniz Institute for Materials Engineering IWT, Laboratory for Precision Machining LFM, Badgasteiner Straße 2, 28359 Bremen, Germany
[b] MAPEX Center for Materials and Processes, University of Bremen, Badgasteiner Straße 1, 28359 Bremen, Germany
[c] Department of Mechanical Engineering, Keio University, Yokohama 223-8522, Japan

ARTICLE INFO

Article history:
Available online 13 June 2020

Keywords:
Manufacturing
Structure
Multiscale

ABSTRACT

Multiscale structured surfaces are a way to provide advanced, otherwise not attainable functionality on a technical part. Applications of such parts can be manifold, and numerous works have already covered the transfer of natural examples into bio-inspired surfaces or the geometrical and functional metrology of such surfaces. After briefly presenting typical functionalities of multiscale structured surfaces, this keynote paper will focus on the available manufacturing processes and review their capabilities to generate multiscale structured surfaces. To compare such processes, the so-called “multiscality” is defined that characterizes the structured surfaces according to the lateral and vertical extent of the individual stacked elements and is used as a first indicator to assess the difficulty of their manufacture. As the boundaries of what is considered a multiscale structure are diffuse, ranges of low, medium and high multiscality are defined instead. After presenting the state of the art of manufacturing processes currently utilized for the manufacture of (not only multiscale) structured surfaces, this keynote paper summarizes the capabilities of single-step and multi-step/multi-physics approaches for their applicability across different scales and gives an outlook on which processes could potentially become relevant in the future.

1. Introduction

The applicability of a technical surface can be significantly improved by introducing surface structures that provide a specific functionality. Many of the functionalities and underlying surface geometries are inspired by nature. Well known examples are the shark skin which inspired the manufacture of riblet structures on airplane wings in order to reduce the drag, the moth eye which was transferred to a micro lens array to enable specific focusing tasks in optical applications, and last but not least the gecko feet which serve as the basis for specific glues and adhesives.

Many of the applications, especially those derived from nature, rely not only on a single type of surface structure, but on a multitude of hierarchically stacked structures. Such surfaces are generally called “bio-inspired” functional surfaces. Looking at the individual elements, it is obvious that their sizes have to differ substantially, or it would not be possible to introduce a hierarchy, i.e. include several smaller structures inside a larger one. To account for this difference in size – which possibly spans serval orders of magnitude – such surfaces are also called “multiscale structured surfaces”.

In the past, numerous publications have covered the topic of functional surface structures. Within CIRP, one of the earliest comprehensive review on the topic has been given in 1999 by Evans and Bryan [42], who gave the definitions on what “structured”, “engineered” and “textured” surfaces are. Nearly one decade later, the keynote paper of Bruzzone et al. [14] provided an update on the state-of-the-art on functional (i.e. typically structured) surfaces in 2008. The more recent keynote papers of Malshe et al. in 2013 [111] and 2018 [112] have focused particularly on bio-inspired structures and surfaces, while Brown et al. reviewed the methodology for the analyses and characterization of multiscale structures [13].

Other past keynote papers addressed the topic from another perspective. Uhlmann et al., for example, generally addressed the manufacturing of high-precision components with microscale features by addressing the associated process chains [160]. Fang et al. also partially covered the topic of manufacturing microstructured surfaces in their CIRP keynote papers on manufacturing and measurement of freeform optics [49] and on nanomanufacturing [48] as well as in another review article on precision injection molding of freeform optics [47]. Furthermore, the recent keynote by Gao et al. focuses on the benefits of on-machine metrology for precision machining processes, which potentially serves as an enabling technology for future surface structuring processes [54].

Complementarily, this keynote paper will focus on methods for the manufacture of multiscale structured surfaces. After specifying the definition of what is understood by a multiscale structure and how its grade can be rated (i.e. determining the “multiscality”), potential applications of multiscale structured surfaces are presented. As the functionality of such or similar surfaces has been discussed recently in the keynote papers of Malshe et al. [112] and Brown et al. [13] this is not a major part of this keynote paper. Hence, only a brief

* Corresponding author.
E-mail address: karpu@iwt-bremen.de (B. Karpuschewski).

https://doi.org/10.1016/j.cirp.2020.06.001
0007-8506/© 2020 Published by Elsevier Ltd on behalf of CIRP.

overview will be given on the functionality. Instead, the main part of this keynote paper will focus on the presentation and discussion of manufacturing processes. It distinguishes between processes that allow for the generation of “true multiscale” structures and those with the potential to generate such surfaces, although it is not directly shown in the referenced literature. Furthermore, sequences and strategies for generating multiscale surfaces (i.e. process chains, hybrid machining etc.) will be discussed.

1.1. Definitions

The term of “structured surfaces” is already well established in the state of the art, referring to *“surfaces with a deterministic pattern of usually high aspect ratio features designed to give a specific function”*, as defined by Evans and Bryan [42]. With multiscale structured surfaces, however, the definitions are not that clear. Some researchers refer to these as hierarchical structures, implying that multiple patterns are stacked [157]. Some also wish to include single layer structures whose dimensions span multiple orders of magnitude in their definitions [84], while others suggest mixing structured surfaces (i.e. geometrically defined elements) on one scale with engineered surfaces (i.e. a deterministic pattern as the result of specific parameters used for the manufacturing process) on another scale [40].

For this paper, multiscale structured surfaces are defined along features as follows: at least two layers of intentionally generated features forming a pattern (i.e. have repeating *or* periodic elements) of different characteristic dimension (lateral *and* vertical) which fully overlap each other with the aim of achieving distinct functions that supplement each other or a combined functionality.

As the term “multiscale” already implies, more than one structure needs to be present and the secondary structure needs to overlap the first one in order to be called a ‘multiscale’ structured surface (Fig. 1, left). Furthermore, the larger structure needs to comprise repeating or periodic elements in order to be justified as a structure, i.e. a free-form surface or a cylinder shape is not counted as a structure (Fig. 1, right), although it is possible to attribute characteristic dimensions to it, e.g. a dominant wavelength. To be distinguishable, the geometric dimensions of the structures need to differ substantially in both lateral and vertical directions. However, their characteristic dimensions do not necessarily have to be on different orders of magnitude, i.e. one on the nanometer-level and one on the micrometer-level. Finally, all structuring applied to the surface has to imply a specific functionality, either independently for each structure scale or as a combined function of structures on all scales.

For assessing and comparing the characteristic dimensions of structured surfaces, significant work has been performed in the field of metrology. Here, the vertical and lateral performance of the instruments defines which structures can be measured and which cannot. Margaret Stedman was the first to characterize stylus instruments according to their capability of measuring specific surface wavelengths and amplitudes. She developed the so-called “Stedman diagram” [145,146] which visualizes the performance range of instruments in the amplitude-wavelength space. The concept was later adopted by Jones and Leach [79], who added a third dimension to the diagram to visualize selected constraints of the instruments for the measurement of surface texture, and by Rosén et al. to include the speed of data collection [132]. Cheung et al. proposed another characterization technique for multiscale structured surfaces [22], which makes use of a priori information on the surface and applies a hierarchical segmentation and registration.

The concept of surface wavelengths and amplitudes can also be used to visualize and compare the range of feature sizes machinable by selected manufacturing processes. In order to assess the manufacturability of multiscale structured surfaces, size ratios in lateral and vertical directions are introduced in this keynote. It is assumed that with increasing size ratios, structures become more and more difficult to machine, as the range cannot be covered by a single process but inevitably requires multi-step or multi-process approaches.

It is assumed that for each structure/manufacturing process presented in the state of the art, the characteristic surface wavelength λ and amplitude a can somehow be extracted. For discrete structures, lateral dimensions (width w, length l) and a vertical extent (height h, normal to the surface) of the features are utilized instead (Fig. 1). If neither of those parameters can be extracted from the given information, statistical parameters, like the peak-valley height Sz or the mean lateral wavelength, are utilized for the calculations in this paper.

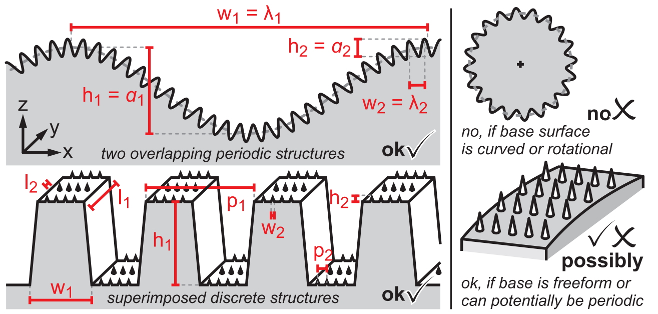

Fig. 1. Characteristic parameters for comparing hierarchical and multiscale structured surfaces.

The two ratios that will be calculated based on the extracted information and used to assess the manufacturability are the “lateral size ratio” n_{lat} (Eq. (1)) and the “height ratio” n_{vert} (Eq. (2)). The first considers the lateral extend (maximum of width w and length l) of the larger structure (s_1) in relation to that of the smaller structure (s_2):

$$n_{\text{lat}} = \frac{\max(w_1,\ l_1)}{\min(w_2,\ l_2)} \quad (1)$$

The height ratio n_{vert} is calculated by comparing the relative heights of both structures. As the structure of the smaller lateral extent may very well be of larger vertical extent than the bigger one (e.g. think of small but long needles applied on top of another structure), maximum height of the stacked structures is compared to the minimum height.

$$n_{\text{vert}} = \frac{\max(h_1,\ h_2)}{\min(h_1,\ h_2)} \quad (2)$$

An exemplary calculation of these parameters is shown in Fig. 2. In the following, these ratios and the respective sizes will be indicated in the presented figures whenever possible. Specific values taken from the references are written in normal typeset; values in *italics* imply that these have been estimated from the respective images (on the basis of the shown scales).

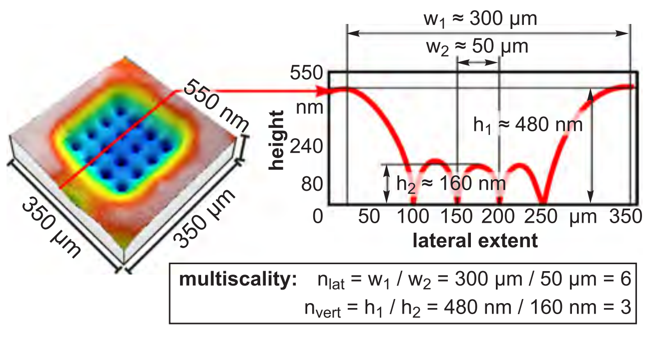

Fig. 2. Exemplary calculation of height and size ratios (calculated for a structure given in [71]).

By evaluating the lateral and vertical size ratios, the extent of “multiscality” of a structured surface and thereby its manufacturing difficulty can be determined. As the review of the current state of the art has shown, both values need to exceed a specific threshold in order to be considered multiscale. In this context, more emphasis is put on the lateral size ratio than on the height ratio. As setting a fixed threshold would not be scientifically justifiable, the following ranges have been defined as “no”, “medium” and “high” multiscality (Table 1).

What this definition does not imply is the pitch p of discontinuous structures or other areal characteristics as well as the general

Table 1
Definitions for the extent of multiscality by a manufacturing point of view.

Multiscality	no	medium	high
Lateral size ratio n_{lat}	≤1	1–10	>10
Height ratio n_{vert}	≤1	1–1.5	>1.5

geometric complexity and the difficulty to control the process during manufacturing. In particular, the relative orientation of the different structure layers to each other is not considered by the definition, because the authors' intention was to establish a basis on which as many examples from literature as possible could be compared to each other, with their scales being the sole basis for that. The definition also does not directly relate to the various possible functionalities of multiscale structured surfaces, because the latter can be attributed to the shape, size and distribution of the structures and are not primarily linked to the manufacturing options.

Overall, as the topic of multiscale structured surfaces is quite broad, the aforementioned aspects must be assessed individually for each of the considered examples. This is done in the discussion of the manufacturing method scalability in Section 4.

2. Application and functionality of multiscale structures

Structured surfaces with multiscale features are utilized in several different applications, mostly to add a specific surface property to a part or to amplify an existing one. Many of these functionalities are often derived from natural examples (Fig. 3). Extensive reviews on this can for instance be found in the 2011 review of Lui and Jiang [105] or in the 2013 and 2018 CIRP keynote papers by Malshe et al. [111,112].

The most common functional properties of bio-inspired surfaces are the adjustment of adhesive properties (gecko feet), the control of the surface wetting state (lotus leaf), improvement of tribological behavior (snake or shark skin) and of course the provision of optical functions such as anti-reflection (moth eye) or color effects (butterfly wings). A strategy for the design of bio-inspired, smart, multiscale, interfacial materials based on these phenomena was proposed by Xia and Jiang in 2008 [166]. The manufacturability of such structures is briefly addressed from a bio-chemical point of view. In addition to the examples derived from nature, there are also some technical examples of multiscale structures that do not directly have a bio-inspired counterpart.

In the following sections, a brief overview on potential functionality and applications will be given. These will be clustered into four groups: structures that are affecting the adhesion of the surfaces to other media (dry-adhesion, hydrophobicity), those that have an influence on the tribology (friction, wear) of contacting surfaces, those that primarily affect the surface reaction to incident radiation (optical functions) as well as any functionality that does not fall into one of these categories (cf. Table 2 for a general overview). Here, it has to be noted that multiscale structures offer the unique possibility to combine multiple functions on one surface, e.g. anti-reflection and self-cleaning. Nevertheless, each function can be typically attributed to a specific structure type.

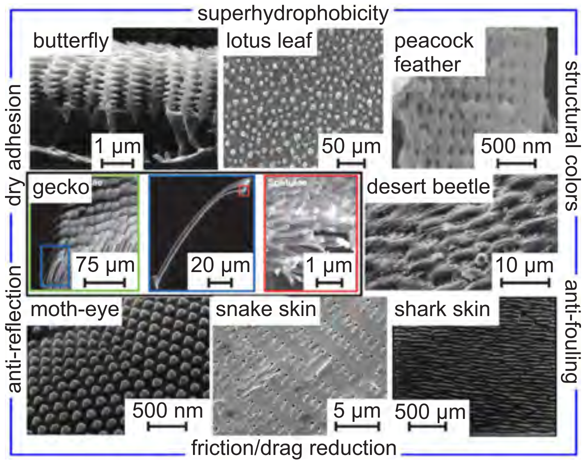

Fig. 3. Biological textures and their functionality [112].

2.1. Properties affecting surface adhesion (wet/dry)

Pthe most prominent examples for bio-inspired multiscale structures are the feet of a gecko, which consist of micrometer-sized hairs with nano-ends on top of overlapping lamellae in the millimeter range [96]. Such structures are adapted in technical products to tune the dry-adhesive behavior of the surface. For this, the size of the applied nanostructures has a larger impact on the adhesive properties than that of the microstructures [184].

Multiscale structures are also frequently applied to control the wetting state of a surface, following the example of a lotus leaf [149]. This concept has, for example, been derived by Asakura and Yan who cut micro grooves into metallic surfaces in order to control the water repellency of the surface [4]. Wang et al. used hybrid nano- and microstructures to significantly improve the hydrophilicity of aluminum surfaces [164]. Kong, Cheung and To designed and fabricated self-cleaning surfaces by mimicking the lotus effect using simplified three dimensional patterned microstructures [92]. Yue et al. showed that the freezing time of droplets on a hierarchically structured silicon surface was four times longer than on uncoated silicon, making such surfaces useful for anti-freezing applications [190]. Rosenkranz et al. demonstrated that multiscale surfaces featuring large structural depths with steep pattern geometries and significantly smaller laser-machined structures (Fig. 4) may be used to stimulate anisotropic spreading of the applied liquids [133].

The surface wetting state obviously also influences the self-cleaning capability of the surface, as hydrophobic surfaces are less prone to

Table 2
Exemplary functionality and structural hierarchy of multiscale structured surfaces .

FunctionalityHierarchy	Surface adhesion (wet/dry)	Tribology	Optical properties	Other functions
single structure; non-multiscale	no adhesion; uncontrolled wettability	improved lubrication and friction, e.g. [67,82,134,156]	microlens array for projection on curved surface [100], multi-aperture [20] or light field [126] cameras	
two superimposed structures	micro and nanostructures for liquid adhesion [184], hydrophilicity [164], self-cleaning [92], anti-freezing [190]		freeform and microlens-arrays for 3D motion detection [125], increase solar absorption [169]; micro- and nanostructure for combined antireflection and antifogging [130], broadband light trapping [3]; nanoflakes and -wires for tunable photoluminescence [162]	nanobushes on nanowires for catalytic surfaces [153], nanowires with carbon nanotubes for stretchable/ transparent electronics [98]
three or more superimposed structures	macro-, micro-, and nanostructures, e.g. for dry adhesion (Gecko) [96]		theoretically possible (e.g. freeform macro lens with micro lens array and nanostructure), but not found in literature	

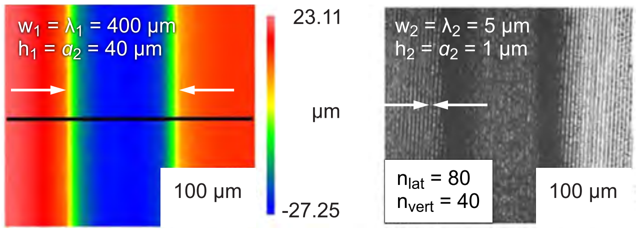

Fig. 4. Multi-scale structured surface for controlled lubricant propagation, adapted with permission from [133].

contamination by dirt and debris, because adjacent particles are repelled. Kong et al. even showed that it is possible to add such self-cleaning properties to transparent polymer parts without severely affecting the optical functionality, making these surfaces multi-functional [92,93].

2.2. Tribological functions

The possibility of controlling the tribological behavior of a surface is another potential function that can be achieved by multiscale structures. Applications in this context are manifold and are primarily found in areas in which two surfaces interact and move relative to each other, where structured surfaces are utilized to reduce friction and wear or improve lubrication [14]. In forming applications, controlling the tribologic conditions of the tool-workpiece-interface by surface structuring or texturing is of particular importance for new developments like micro or dry metal forming [17].

For instance, Karpuschewski et al. indicated the potential of cylinder liner surface engineering by honing for improving the efficiency of combustion engines [82]. Hense et al. showed that high feed milling may be utilized to generate structured forming tools with exhibited anisotropic friction coefficients and thereby can be used to direct the material flow during sheet-bulk metal forming [67]. Tillmann et al. compared thermally sprayed surface in their unmodified state with coatings structured by micromilling, which featured dimples as well as structures inspired by the scarab exoskeleton [155]. They found out that the dimple structures lead to a significant reduction of friction and wear, but were surpassed by the bio-inspired (scarab), i.e. multiscale, structured coatings (Fig. 5). However, the burr resulting from subsequent treatments of a surface may increase friction and adhesive effects [156].

The influence of different structures and textures on sheet-bulk metal forming was experimentally and numerically analyzed by Kersting et al. [83] and utilized for developing tailored surfaces and process strategies for incremental forming processes [108,143,144]. Furthermore, the impact of the structuring on the subsurface damage has been in focus of subsequent analyses [109].

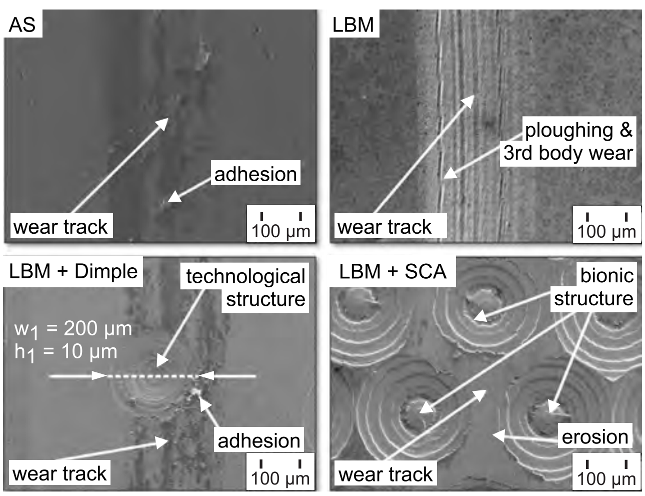

Fig. 5. Wear tracks on as-sprayed (AS), laser machined (LM), technologically (dimple) and bionically structured (SCA) coatings [155].

Structuring of surfaces may also affect sliding conditions due to the formation of pockets on the surface that entrap the wear debris or patterns with simply reduce the sliding contact area [63,150,152]. Gnilitskyi et al. have shown that nanopatterning by nonlinear laser lithography is capable of friction reduction in both dry and lubricated sliding conditions, with the orientation of the nanostructures having a significant influence on the decrease under dry conditions [57]. Rosenkranz et al. fabricated hemispherical structures with different area densities by microcoining and demonstrated their effect on the friction reduction under mixed and full film elastohydrodynamic lubrication [134]. Hermann et al. showed that a combination of sinusoidal waves and coatings is suitable for enabling dry metal forming with rotary swaging processes [68]. The reduced friction and wear is also beneficial for cutting operations, as shown by Xing et al. who used textured cutting tools in dry cutting of aluminum [171].

2.3. Optical functions

Optical functionalities are one of the most exploited applications of multiscale structured surfaces. The use of lens arrays can, for example, provide an optical system with new possibilities for system design and performance. For example, Li and Yi showed that freeform microlens arrays may be used to construct an ultraprecision 3D projection lithography system (Fig. 6) that allows for the structuring of curved substrates with a projection ratio of 34:1 compared to the structures defined on the mask [100].

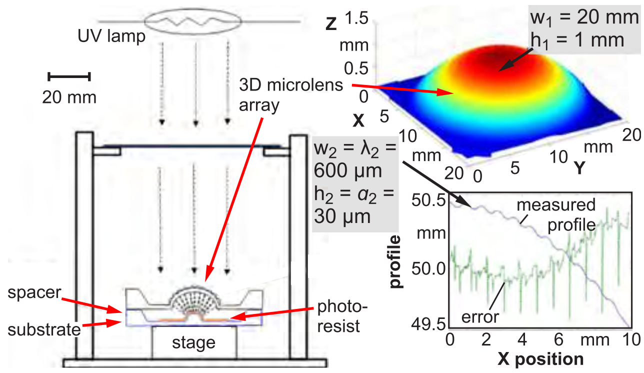

Fig. 6. 3D projection lithography system using a freeform microlens array as developed by Li and Yi, adapted with permission from [100].

Chen et al. showed that multiple apertures may be realized in one camera setup [20] by implementing freeform microlens arrays. These allow for a wide field of view while maintaining a thin and compact camera setup, as they verified using raytracing simulations. Pang et al. designed and fabricated a light field camera using overlapping microlens arrays [126] for which they claim that a shorter fabrication time and cost is required compared to tangent microlens arrays. With their novel design, the fill factor of the light field was increased 1.24 times. They later also designed and manufactured a bionic compound eye for 3D motion detection using the principle of freeform surfaces and microlens arrays [125].

When superimposed by hierarchical (nano) structures, these optics may be endowed with additional properties. Yang and Aizenberg presented strategies for fabricating microlens arrays with integrated pores that enable biomimetic hybrid optical systems with tunable properties [183]. Raut et al. have shown a method to produce optics with improved performance in terms of light sensitivity and the added benefit of the surface being self-cleaning [130]. For this, they first imprinted anti-reflective structures on a flexible polycarbonate substrate, then coated a sacrificial layer on top and finally imprinted the microlens array into the composite. After washing the substrate, the sacrificial layer was removed, and a hierarchical surface is obtained. This reduced the reflectance of the micro lenses down to about 5% (Fig. 7). Further improvements, down to 1.4% were achieved when nanostructures were not only applied on the lenses, but also on the flat backside of the glass substrate.

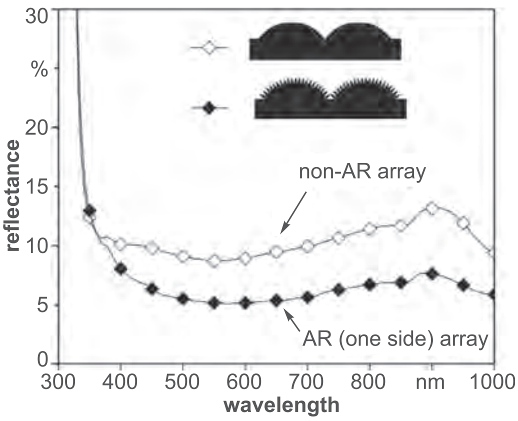

Fig. 7. Reduced reflectance achieved by superimposing nanostructures on microlens arrays. Adapted with permission from [130]. Copyright (2015) American Chemical Society.

This entrapment of light is also beneficial for solar power applications in which the majority of the inbound sunlight needs to be absorbed by the panels. Han et al. demonstrated in [61] that periodic nanopyramid structures machined on germanium substrate are capable of achieving a 100% absorption across a broad band of wavelengths (500–800 nm). Anguita et al. showed that a nanostructured graphene layer sputtered on a surface allows a similar absorption from the mid-infrared to the ultraviolet range [3]. Xie et al. showed that the efficiency of solar panels may be increased by shaping the glass substrate covering the solar cells into a curved shape and structuring it with microlenses [169]. This increases the absorptivity by 3 to 3.4% and thereby enhances the average power conversion efficiency.

Multiscale structures may also be used to enable superfocusing, i. e. focusing beyond the diffraction limit, in optical systems. Fu et al. have shown that chirped circular nanoslits (slits with varying widths and period) may be used to construct such plasmonic lenses [51]. Liu et al. later compared the performance of plasmonic lenses with varying slit width, slit depth and hybrid lenses with width and depth varied at the same time [107]. They found that the pure variation of the slit width achieves the best focusing performance.

Concerning optoelectronic devices, Wang et al. have shown that synthesized nanoflakes and hybrid nanoflake-nanowire structures may be utilized to tune the photoluminescence optical modulators or filters [162].

2.4. Other technical functions

Apart from the aforementioned functions that are achievable with multiscale structured surfaces, there are other applications in electronics, material design or bioactive surfaces that rely on a hierarchical structure of some kind. Although not in the main focus of this keynote, two applications will be briefly covered here, as the processes used for their manufacture might also be relevant for the structuring of other surfaces.

Ta, Park and Noh demonstrated the fabrication of zinc oxide nanostructures (“nanobushes”) on the surface of silver (chemical symbol Ag) nanowires (Fig. 8) which may be used to improve the photocatalytic performance of a surface, i.e. the ability to degrade organic material when illuminated by (sun)light, and is used for water or air purification, waste treatment or asepticism [153].

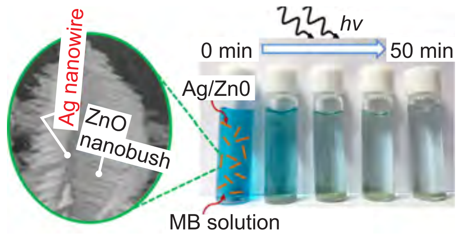

Fig. 8. ZnO nanostructures on Ag nanowires for improved photocatalytic activity [153].

Lee et al. developed hierarchical multiscale hybrid nanocomposites comprised of silver nanowires and carbon nanotubes which can be used to fabricate conductors that are highly stretchable or transparent and thus are specifically favorable for a usage in wearable electronics [98].

3. Capabilities of manufacturing processes to generate structured surfaces

The manufacture of structured surfaces can be achieved by a variety of different processes and diverse manufacturing principles (Table 3). In this section, an overview on current capabilities will be given along with examples of machinable structure geometries, size ranges and specific potentials and limitations the respective technologies might have, e.g. efficiency in terms of areal generation rate, applicability to certain workpiece materials.

3.1. Cutting

3.1.1. Milling processes

Conventional milling is one of the most frequently used processes for material removal throughout the world. Regarding the topic of this paper milling is very often the chosen process to machine large scale structures on workpiece surfaces that are later on superimposed

Table 3
Manufacturing principles and processes for structured surfaces with characteristic structure types and sizes range.

#	Manufacturing principle	Process	Examples for typical structure types	Size range
3.1	Cutting	Milling processes	textures [6,7,142], dimples [34,38,89,117], grooves [12,44,140], pyramids [167]	µm to mm
		Diamond milling / fly cutting	grooves [10,43,45,205], pyramids [157,216], cavities [182]	nm to mm
		Turning processes	Fresnel structures [75], lens arrays [206], grooves [91], gratings [53], diffractive pattern [118,119]	nm to mm
		Vibration assisted texturing	nano-texture [59], wave pattern [195]	nm to µm
		Planing, grooving and chiseling	grooves [180], prismatic cavities [10,11,74]	µm to mm
3.2	Abrasive machining	Grinding	riblets [29,35,37,39,101], pyramids [170], linear lens array [197]	µm
		Polishing	cavities [41], micro lens arrays[106]; post processing of structures in general	mm
		Honing	honing structures, lubrication pockets [25,82]	sub mm
3.3	Forming processes	Nanocoining	micro channels [177,210], pockets/dimples [134,152,188], plateaus [77]	µm
3.4	Beam based processes	Laser beam machining	pockets [16,188], wave pattern [133,136], gratings [55,56], textures [124,135]	µm
		FIB direct writing	gratings/masks [46], nanolenses [52], nano-steps [174], DOE [176,202]	nm
3.5	Electrical machining	EDM, ECM	stochastic pattern [211], pockets [198], channels [72], pins/needles [24]	µm
3.6	Lithography	Photolithography, direct patterning lithography, nanoimprinting	gratings/masks [114,127], dimples [63,97], lens arrays [80,87,130,158,183], grooves[19], spikes/needles/pins [40,78,129], foams/porous pattern [64,164]	nm to µm
3.7	Chemically assisted manufacturing	Etching	texture [131,194], terrace and leaf structures [85,189]	nm to µm
		Chemical synthesis	masks [60], fibers/wires [23,94,153], pits [8], needles [18], lamellae [172]	nm to µm
3.8	Other processes	Replication processes	negative of mold shape, needs to be demoldable	nm to mm
		Self-assembly	molecular structures and arrays [69,70]	nm
		Additive manufacturing	porous and matrix structures [2,60], pyramids and micro lenses [192]	µm to mm

by microstructures with dedicated features made by many different techniques. Very promising examples of these combinations can be found in the area of tool surface modification for metal forming. Either in deep drawing or in sheet-bulk metal forming (SBMF) attempts have been made to improve the frictional behavior between tool and workpiece material by applying dedicated surface modifications to the tool i.e. the die. Although most of the published work so far does not fulfill our definition of a true multiscale surface it is worth mentioning these approaches, because they bear the potential to generate these true multiscale surfaces.

A group from Dortmund made use of self-excited tool vibrations to create specific workpiece surfaces [7]. Most often this phenomenon called “chatter” is avoided due to uncontrollable results and instable conditions, however it can be used to produce ornamental surfaces in woodworking (“chatter turning”, see e.g. [147]). The major benefit of their work is the chance to predict the generated surface pattern based on eigenfrequencies of the tool with a suitable process simulation based on Constructive Solid Geometry techniques. Results show reasonably good agreement between simulation and experiment, but so far the application was limited to plane surfaces. Another way to modify the surface of tools for SBMF is to combine high-feed milling with subsequent PVD coating [6]. With $n_{vert} \approx 1.5$ and $n_{lat} \approx 2.5$, this is again no generation of a true multiscale surface, but the authors could show a shift in the surface characteristics after the milled structures were coated. Even without coating the approach of using high-feed milling is able to generate tailored surfaces of punches for metal forming by changing the friction coefficient of the (not multiscale) surface [66].

The adapted modification of die surfaces can even lead to lubricant free deep drawing processes. Brosius and Mousavi could prove that they can calculate the necessary non-flat macro geometry of blank holder and drawing die to allow dry processing of sheets in deep drawing [12]. Although, no specific emphasis was placed on the manufacturing of these macro geometry surfaces by cutting, this reference is included due to the geometrical modeling involved.

If a fast tool servo (FTS) drive is added to a conventional milling spindle, many different patterns can be generated on the workpiece surface. Denkena, Köhler et al. have shown how to calculate and realize different patterns on an aluminum surface [36,89]. Results shown so far reveal the potential of generating real multiscale surfaces, Fig. 9.

The topic of friction reduction is also enabled by dimple structures to machined surfaces. Dimples are used as oil reservoirs and micro bearings. Denkena et al. have shown, that fly cutting of dimples can largely influence the friction coefficient of cylinder liners [34,38]. Instead of fly cutting these micro dimples can also be generated by two-flute ball end mills in a mill-turning kinematic [117]. If the depth of cut is less than the tool radius the surface can be generated very fast with a minimum of non-cutting time.

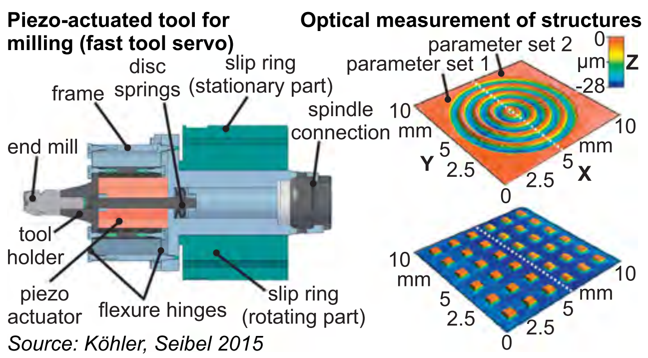

Fig. 9. Micro structure generation with a fast tool servo in milling, cf. [89].

A special variant of cutting with a well-defined cutting edge is whirling. Matsumura et al. have shown, that it is possible to generate dimples on a cylinder by indenting the tool geometry into the workpiece surface without chip removal just by adjusting the rotational speeds of tool and workpiece and the related eccentricity accordingly [116]. The authors have shown that with the kinematic interaction of whirling even thin wires of less than 1 mm diameter can be structured with micro threads [140].

A real multiscale surface according to our definition can be generated if an additional micro-cutting-edge array is applied to macro ball end mills [167]. By micro grinding a specific cutting edge pattern was applied to tungsten carbide based ball end mills of radius 6 mm and 1.5 mm respectively, Fig. 10 top. Both tools were used to generate different types of microstructured surfaces, the larger tool for micro pyramids (Fig. 10 bottom left), the smaller tool for a micro pyramid array on an aluminum freeform surface (Fig. 10 bottom right). Taking the approximate lateral wavelength and height of the underlying freeform into consideration, this accounts for multiscality values of $n_{lat} = 125$ and $n_{vert} \approx 80$.

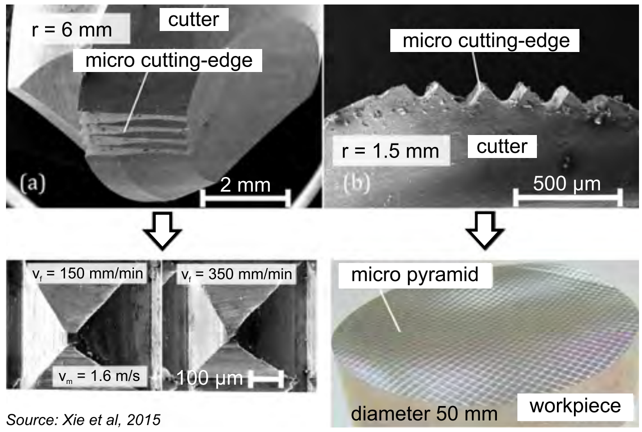

Fig. 10. Micro structured surfaces by using macro tools with micro edge arrays [167].

For micro structuring of surfaces micro milling is often applied. In this case tungsten carbide based milling tools with diameters of less than 300 μm are used. Fang et al. presented investigations on the rigidity and performance of different micro mills to be used for micro structuring [44]. In [142] micro mills of 300 μm diameter were used to structure the surface of tools for incremental bulk forming. A bio-inspired surface (scarabaeus beetle structure) was applied by micro milling. After that the tool was PVD-coated. Forces, frictional and tool-related deformation could be reduced by applying this tool surface modification, although again it is not a multiscale surface.

3.1.2. Diamond milling / fly-cutting

Diamond milling processes, often also termed as fly-cutting are one of the most flexible and efficient processes in ultra-precision machining. With the diamond tool rotating and the workpiece being moved relatively slowly on a numerically controlled path a wide range of products can be manufactured. Due to the various milling processes available, there is a large number of possibilities for machining complex shapes and structured surfaces. Despite the vast flexibility and the theoretical possibility for generating structured surfaces not many examples for multi-structured were found; diamond milling is mostly applied for structuring planar or basic curved surfaces. But in general a secondary structure could be superimposed by structured cutting edges of the diamond tools or subsequent milling processes.

Fly-cutting of micro V-grooves is a typical milling process which is widely used for optical fiber positioning, retro-reflection, for optical gratings or other light guiding applications. Zhang et al. have demonstrated this but with focusing on the improvement of the machining accuracy by on-machine metrology of the tool alignment [205]. As the technique is used for generating a single structure and not for the generation of multiscale structures, multiscality values cannot be calculated in this case.

The application of fly-cutting for hydrophobic purposes has been demonstrated by Brinksmeier et al. [10], who machined intersecting V-grooves into molds for polymer replication. Even though also here no multiscale structures have been generated the capability of covering a variety of scales and thus steering the functionality is shown according to the parameter for structure spacing s which can be controlled from the single micrometer range to hundreds of micrometers (see Fig. 11).

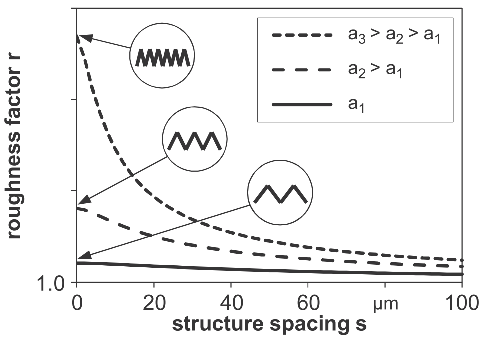

Fig. 11. Dependence of roughness factor *r* on structure spacing *s* and aspect ratio *a* [10].

Ball-end milling with single-crystalline diamond endmills has been applied by Yan et al. to fabricate microstructured surfaces exhibiting dimples and grooves [182]. Besides the machining of dimple arrays and micro-pyramids generated through intersecting grooves a surface generation model is shown which demonstrates a secondary surface structuring of grooves by microstructured cutting edges. Here, the wear pattern of worn diamond tools is replicated into the machined surface (see Fig. 12), but intentionally structured cutting edges might be applied for the generation of multiscale structured surfaces.

Another also unintentional structuring effect was investigated by Fang and Liu [43]. Burr formation is a problem occurring when micro cutting or milling of e.g. retroreflective structures. Experiments were carried out in brass by fly-cutting with a single crystal diamond tool; fly-cutting was chosen because it delivers a nanometric undeformed chip thickness over a large range of cutting speeds. Nevertheless, exit-burrs are formed even if the undeformed chip thickness is down to a few nanometers. Thus, instead of attempting to eliminate burrs, effort should be made to minimize them.

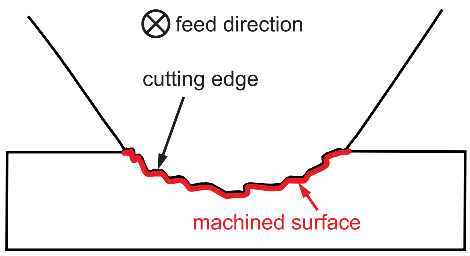

Fig. 12. Secondary surface structuring in fly-cutting by microstructured cutting edges [182].

The investigation shows that exit-burrs can be minimized through optimizing the cutting parameters where cutting speed only has a minor effect, while undeformed chip thickness affects the height of the exit-burrs significantly. The amount of burr formation was further demonstrated by Fang et al. for fly-cutting of step-mirrors for laser-diode beam shaping [45]. Here, again, cutting speed showed a negligible influence while the feed mode (up /down hill) is decisive and burr height could be reduced from 5 μm down to 0.5 μm. Both examples have in common that burrs represent imperfections of the machined surface, but if generated in a controlled way might be regarded as multiscale structures.

Diamond machining for the deterministic generation of hierarchical micro nanostructures has been implemented successfully by To et al. [157] and Zhu et al. [216]. Here a novel system and process was developed by combining fly-cutting with four-axis servo motions with fast/slow tool servo diamond machining. A complex shaped primary surface is generated by material removal, while the desired secondary nanostructures are simultaneously constructed using residual tool marks by actively controlling tool loci. The potential was demonstrated by fabricating a nanostructured F-theta freeform surface and a nanostructured microaspheric array (MAA), see Fig. 13.

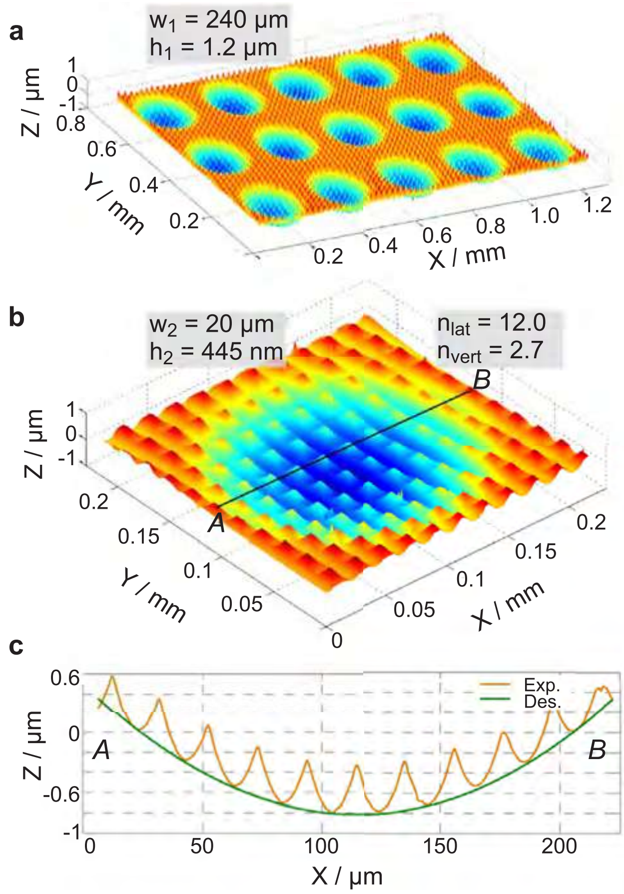

Fig. 13. Characterizations of (a) the microaspheric array (MAA) with nano-pyramids; (b) a single microaspheric structure with nano-pyramids; and (c) the enlarged view of the secondary nano-pyramids [157].

The aperture of each micro aspheric structure was 200 μm, the distance between two successive structures 250 μm and a height of 1.2 μm; the secondary structure generated, i.e. nanopyramids, reveal a nominal height of 445 nm at a pitch of 18.5 μm. These leads to a lateral size ratio n_{lat} = 250 μm / 18.5 μm = 13.5 and a height ratio n_{vert} = 1.2 μm / 0.445 μm = 2.7, respectively. According to our definition the multiscality can be rated as high for both dimensions.

The optical effect of such a multiscale structured surface is illustrated in Fig. 14. A qualitative investigation method was applied showing on a screen that the diffractive light pattern obtained from the freeform surface with nano-pyramids (FFS-NP) is uniformly

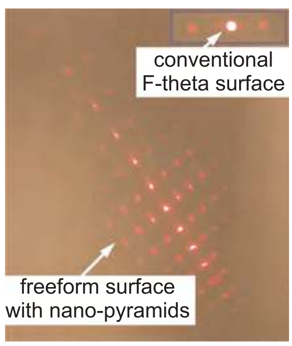

Fig. 14. Reflective diffraction of the freeform surface with nano-pyramids (FFS NP) [216].

distributed with nearly equal spacing compared to the conventional surface which exhibits only one reflection spot with two first order diffraction spots.

3.1.3. Turning processes

Turning processes are characterized by a high degree of flexibility with respect to the achievable geometrical shapes, a high structuring quality with low surface roughness as well as the high processing speed [53]. These features make the process particularly suitable for the production of complex geometries such as sinusoidal gratings [53], Fresnel lenses [181], micro lens arrays [206] or non-rotational symmetric freeform surfaces [90]. However, turning processes are equally suitable for the machining of multiscale surface structures. The various machine configurations and available axes as well as the different process variations like longitudinal or face turning, are allowing the machining of a multitude of different geometries.

An example of multiscale structures generated with turning is the structuring of roller-molds. The machining of this circumferential surface of the cylindrical roller results in a first regular surface geometry in the scale of the radius of the roller, which is superimposed by the individual structuring of smaller surface structures, like V-groove gratings [104]. The linear and rotational axes available on the respective machine tool can be used to expand the variety of machinable geometries or to improve the imaging quality of the structure, depending on the application, resulting in a relatively low level of multiscality. Huang et al. [73,75,204,208] for example use the B-axis of the machine tool to rotate the diamond tool. Doing so, they can machine the deep circular grooves of a Fresnel lens on the periphery surface of the roller mold in all rotational directions. Another way of creating multiscale structures on the circumference of a roller is to vary the feed depending on the radial positions of the spindle [91]. In this way, wavy grooves are created in the periphery of the roller, which will form various geometric shapes when they are overlaid, as shown in Fig. 15.

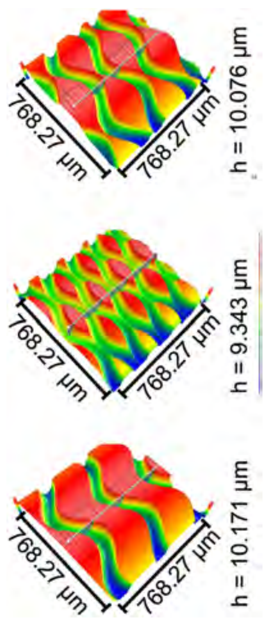

Fig. 15. 3D topography on the roller surface after cutting with varying feed [91].

To increase the scope of machining and thus the multiscality of the surface structure, the machine's own axis systems can be combined with external high-frequency actuators. Especially for the machining of non-rotationally symmetric surfaces, like microstructures as well as arbitrary freeform surfaces, additional axis can be valuable. In his review on Fast Tools Servo (FTS) systems, Zhu, Li et al. [213] give an extensive overview on FTS machining with high-frequency response (work frequency of several hundred Hertz up to several Kilohertz), comparing different systems regarding structural characteristics of the machining processes, control algorithms and tool path planning (cf. Fig. 16).

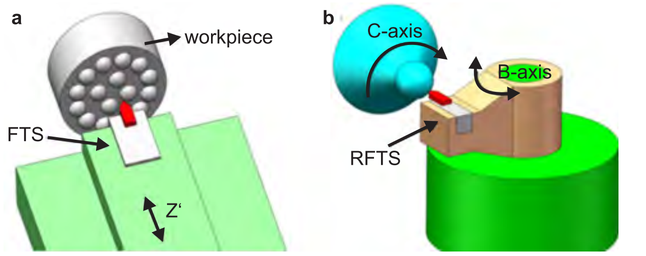

Fig. 16. a) Linear FTS turning of a micro lens structure. b) Rotary FTS turning of a target ball microstructure [213].

The great potential of FTS machining for the improvement of surface quality and the extension of the degrees of freedom inherent in the process has been proven in many publications. Examples for the machining of complex optical microstructures, like security holograms, is given by Meier et al. [118,119]. They use a nano Fast Tool Servo with a stroke of up to 1000 nm and a working frequency of 5 kHz in combination with an ultra-precision tool lathe for the structuring of diffractive optical elements on a flat surface. This process represents a cost-effective and fast solution to produce diffractive surfaces in a single process step and is therefore able to replace the conventional production by lithographic processes.

Another example is the application of a Fast Tool Servo for the compensation of machining errors of the Slow-Tool axes in-line, thus during the machining process [121]. By using advanced combinations of the machine slow-tool axis with high frequency fast tool axes, the resulting superposition of long-wave and short-wave movements can be applied for the structuring of micro lens arrays on curved surfaces such as spherical sections [100,203], or even freeform surfaces [22,90,214] (cf. Fig. 17).

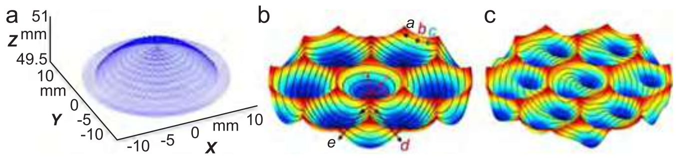

Fig. 17. a) Toolpath of the designed 3D micro lens array for the slow tool servo process [100]. b) Conventional spiral path based fast tool servo diamond cutting of a microsphere lens array and c) a microfreeform lens array [214].

In comparison to the previously described FTS-supported turning, in which the axis movement is performed in a controlled manner with defined deflection steps, FTS-systems can also be used for micromechanical texturing [58]. By oscillating the diamond tool during the cutting process, micro dimples are generated on the workpiece surface. This setup can be adapted to different machining strategies like the texturing of the inner or outer diameter of a cylinder or in a face turning process.

3.1.4. Vibration assisted texturing

Those former cutting processes can be modified to better fit the purpose of texturing surfaces. As Yuan et al. [188] proposed, sophisticated surface topographies with designed micro/nano-structures can enhance the functionality and performance of products. Some possibilities are the influence of the anisotropic wetting behavior, the hydrophobia or the friction behavior of a surface.

One modification of the conventional cutting processes to generate those micro/nanostructures is the vibration assisted cutting. The idea behind this process is based on the specific overlay of two movements of different scales. For example Denkena et al. [31] used a piezo-electrically driven milling tool as a fast tool servo (FTS) to mark products during a face milling process. While not gaining specific mechanical improvements on the surface, this method shortens the process chain, as a separate marking process is not necessary.

Hense [66] by contrast used the chatter vibrations of the machine to overlay two movements of a different scale. He demonstrated that during a milling process intentionally invoked chatter can create tribologically effective surfaces, although this purposeful chatter requires a precise understanding of the dynamic characteristic of the machine and process respectively.

Another approach is the ultrasonic assisted turning investigated by Suzuki et al. [151], as well as Moriwaki and Shamoto [120]. Compared to a conventional turning process the tool additionally vibrates with a high frequency along an elliptical shape (Fig. 18). This reduces tool wear and adhesion, as well as brittle fractures on the generated surface.

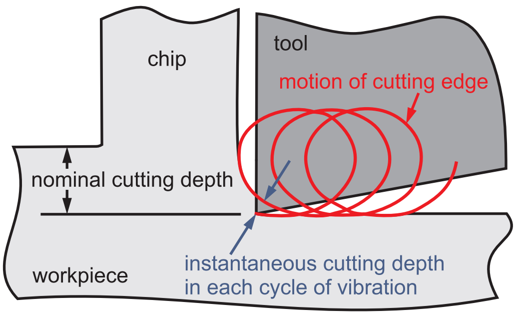

Fig. 18. Elliptical vibration cutting process, according to [151].

In contrast to turning, where the vibrating tool remains at a fixed position while the workpiece is rotated, Xu et al. developed a method called rotary ultrasonic texturing (RUT) in which the spindle and thus the rotating tool is set to oscillate at a specific frequency [173]. The proposed method allows for the vibration to be directed in different directions, e.g. linearly along the rotor axis, perpendicular to it or in a mixed fashion to create circular or elliptic motions. In combination with the feed direction and velocity, this enables various textures to be applied to a surface.

The generation of multiscale structured surfaces with this method was investigated by various researchers. Guo et al. used the ultrasonic assisted "elliptical vibration cutting" (EVC) to generate a first-order microstructure with a superimposed second-order microtexture on aluminum surfaces [59]. The addition of those textures resulted in a nearly doubled anisotropic water contact angle. In addition, Zhang et al. changed the amplitudes of the elliptical shape and concluded, that the machinable part geometry is mostly restricted by the cutting tool geometry and the vibration conditions [195]. They confirmed that the process can achieve structures with a step height of more than 2 nm and a pitch of more than 250 nm with an accuracy of 1 nm. Later they optimized this method with further error compensations and verified that it can be used to generate nano-structures with a large ratio of structure height to wave length [196]. Zhu et al. utilized a technique in which they combined rotary special vibrations (RSV) of a diamond tool with slow servo motions of the workpiece to generate micro- and nanostructures of varying complexity [215].

In summary, vibration assisted texturing can be used for manufacturing lower scale structures, while for multiscale surfaces the larger structures remain to be generated by the underlying conventional machining process.

3.1.5. Planing, grooving and chiseling

The production of linear, prismatic and discontinuous optical microstructures such as micro grooves, micro pyramids or micro lenses is becoming increasingly important in optic design. By machining these microstructures into nickel phosphorous (NiP) coatings, they can be used as molds and are applicable to glass molding processes as Yan et al. investigated [180]. For these grooving processes, the machining process has to be optimized to minimize material adhesion and occurring burrs (Fig. 19). Often the process is separated into incremental steps to reduce the undeformed chip thickness and therefore the cutting forces.

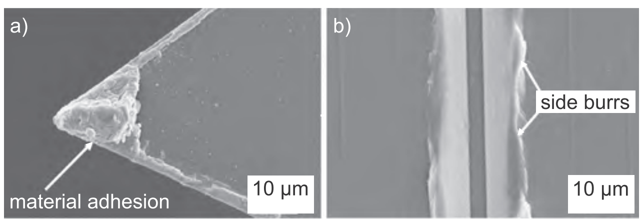

Fig. 19. SEM photographs showing a) material adhesion on diamond tool and b) microgrooves with side burrs. [180].

Sun et al. [150] demonstrate the manufacture of V-grooves with ridge angles of 60°–90° and heights between 20 and 50 μm which may be applied to surfaces for friction reduction. Even smaller groove structures were fabricated by Takayama, Ishizuka and Yan, who utilized single crystal diamond tools with a cutting edge structured by a picosecond pulsed laser [154]. The microgrooves on the cutting edge featured a depth of 9 μm and a spacing of 6 μm and were evenly distributed along a 1.1 mm wide straight cutting edge. Using this cutting tool at a set inclination angle to the workpiece surface, hierarchical structures, i.e. 264 μm wide grooves with a 6 μm wide and 9 μm deep substructure, can be generated.

Despite the superb usability for groove structures and gratings, conventional turning and milling processes often lack the ability to produce defined discontinuous structures, as they are for instance required by corner cube retroreflectors. For this purpose, Brinksmeier et al. have developed the diamond micro chiseling (DMC) process [10,11]. Using V-shaped diamond tools and dedicated kinematics (Fig. 20), this process enables the machining of prismatic cavities with facet angles of 30° to 54°

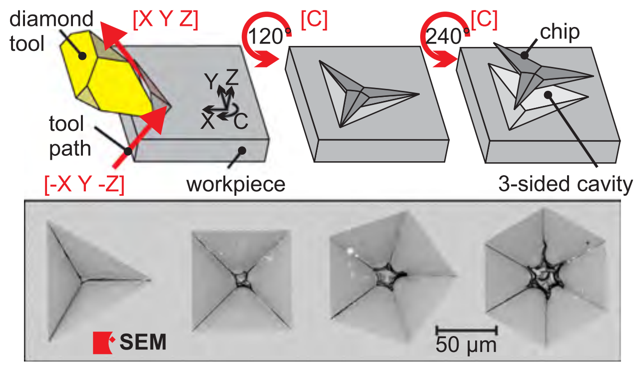

Fig. 20. Diamond Micro Chiseling, process kinematics and achievable structure geometries [10].

The achievable structure size is dependent on various parameters, including workpiece material, number of facets in a cavity and structure angle, and typically ranges between 15 μm and 1 mm (facet width in top view). Complex patterns can be formed by overlaying multiple cavities. Recently, the process was extended to also machine structures on curved substrates [137].

A similar technique, which also relies on the use of a V-shaped sharp diamond tools and a multi-axis ultra-precision machine tool (Fig. 21), was developed by Huang et al. [74]. The so-called diamond

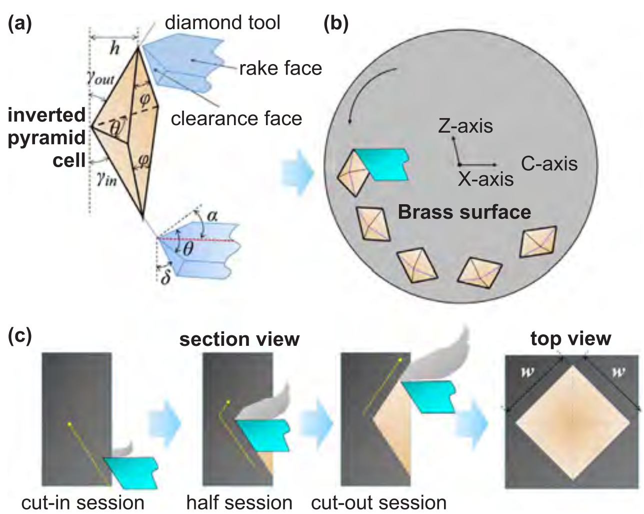

Fig. 21. (a) Geometrical dimensions of engraved cells and the respective cutting tool, (b) Machined inverted pyramid features along the tool trajectory, (c) Motion study of micro engraving in a three-step section view. [74].

micro lithography (DML) is used for generating grayscale micro images on metal surfaces as a potential anti-counterfeiting technique. This method is capable of transferring a given grayscale image onto a metal surface by generating inverted pyramids on an Archimedean spiral tool path for different image sizes. Due to the changing effective rake angle from the cutting in section to the cutting out section, some burrs and shape distortions occur on the surface.

The change of rake angle is also crucial in the machining of gratings and diffractive optical elements (DOE) by ultra-precision machining [99]. Uhlmann et al. also investigated this issue for the machining of DOE for variable rake angles and thus for variable chipping conditions in the sagittal plane [159]. They discovered that the influence of the rake angle on the surface roughness is dependent of the investigated material. Nevertheless, for applications with wear susceptibility a tracking of the sagittal slope could be advantageous to reduce process forces and tool wear (Fig. 22).

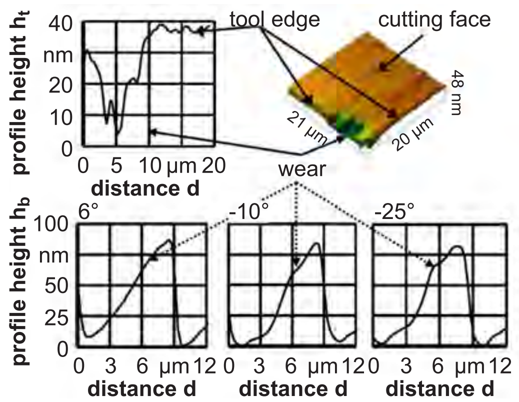

Fig. 22. Wear profile of the tool edge (top), effect on the nanostructure (blazed grating) dependent of the sagittal slope (bottom). [159].

3.2. Abrasive machining

3.2.1. Grinding

Grinding is used mainly for surface structuring of difficult-to-cut materials. Fig. 23 shows a grinding wheel with a patterned topography fabricated by fly-cutting. Experimental results showed that the patterned grinding wheels significantly decreased the mechanical and thermal loads in the contact zone [27,28,33]. Moreover, a grinding tool with two different grain sizes was developed to fabricate the plateau like surface to reduce friction and create an oil reservoir to improve the fluid film stability [30].

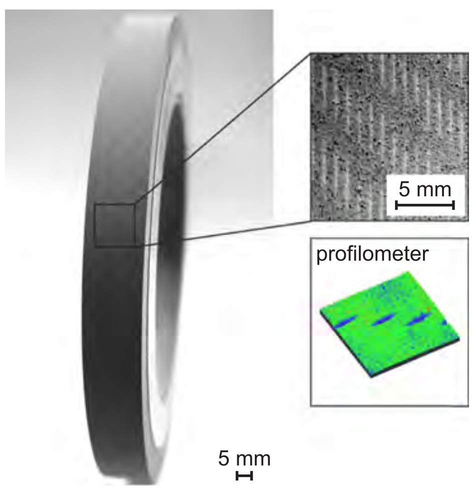

Fig. 23. A surface-patterned grinding wheel [27].

The small grains generate a smooth surface and large grains generate deep grooves. Furthermore, by using a sharpened diamond wheel

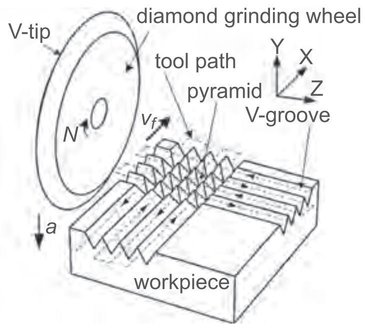

Fig. 24. Grinding for micro pyramid structures [170].

with a V-tip, microgrooves were fabricated on the rake surfaces of cutting tools to decrease chip-tool frictions and excluding cutting heat [168]. Fig. 24 shows the fabrication of micro pyramid structures by crossed grooving with a V-tipped grinding wheel [170]. It was also used to fabricate a 400 μm deep microlens array on a macro-freeform glass substrate for amorphous silicon thin film solar cells [169,197].

Ground microstructures can be used to improve the tribological performance of surfaces, and to reduce flow losses or even to store information [32]. Extensive work has been done on manufacturing of riblet structures on compressor blades with the purpose of drag reduction in turbulent flow [29,35,37,39,101]. In addition, ultraprecision grinding was used to generate small-aperture concave aspheric surfaces on tungsten carbide material. The generated surface has high accuracy of PV $\approx$ 100 nm and surface roughness of Ra $<$ 10 nm [178].

3.2.2. Polishing

Polishing typically does not generate a structured or multiscale surface by itself, but is used to smoothen an existing surface, e.g. the faces of a previously generated microstructure. This, however is a challenging task, as it requires dedicated alignment strategies and non-traditional methods for generating the polishing motion. For instance, an experimental setup for polishing millimeter-sized retroreflector facets was developed by Elsner-Dörge et al. and its stability was proven by experiments [41]. Another example is abrasive flow polishing, which can also be applied to micro structures, such as bores [185].

Nevertheless, the direct generation of structured surfaces by polishing techniques is possible. Huang and Yan, for example, used polishing and subsequently nanoindentation to generate multiscale dimples on metallic glass [71]. In order to efficiently fabricate microlens arrays on a hard mold surface, a unique method of lapping/polishing by employing precision balls and diamond slurries was developed by Liu et al. [106]. As shown in Fig. 25, precision alloy steel balls were implemented to shape the microlens cavity to an approximate depth that was very close to the required sag value and then plastic balls were applied to polish the surface to optical surface quality. This method is also used to fabricate microlens arrays on non-planar surfaces in optical applications [106].

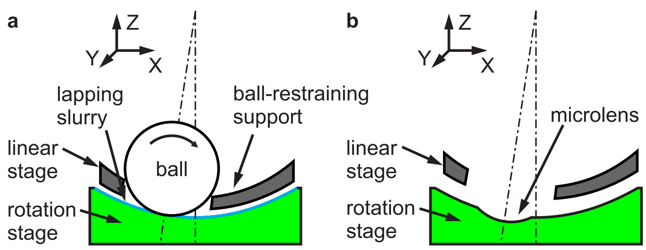

Fig. 25. Schematic of lapping/polishing method for structured mold fabrication, according to [106].

3.2.3.Honing

Honing can be defined as an interaction of mechanical work and physical chemical processes. Micro-hardness, residual stresses, lattice structure and chemical boundary layers define the surface integrity and can be seen as a function of honing process parameters and running-in conditions [82,165].

Micro-structuring of cylinder liners can reduce friction in combustion engines. The honing operation of cylinder surfaces is an important step in engine production. In industry attempts have been made to structure the honed surface in highly loaded areas by applying laser structuring afterwards [1]. But due to blown out melting particles a final honing step had to follow. As one alternative a hybrid tool consisting of a honing unit and a fast tool servo driven by a piezo actuator was developed for machining cylinder liners with micro-scale features.

Fig. 26 shows examples of two different workpieces after pre-honing and structuring. The hybrid cutting tool is up to 6 times faster than laser structuring for structuring grooves [25].

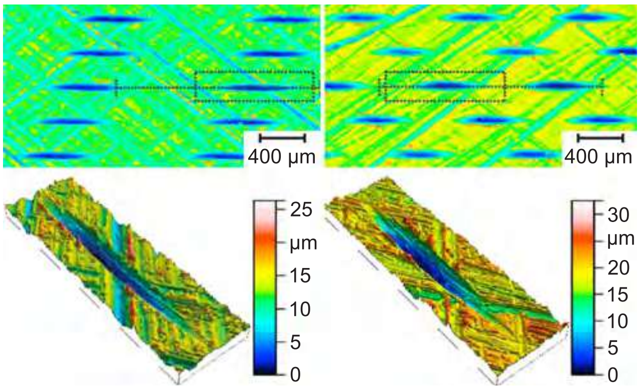

Fig. 26. Cylinder surface with prismatic inserts by honing [25].

Researchers from Magdeburg have used an alternative approach to structure the cylinder liner surface similar to a laser structuring [81,82,165]. They applied a micro structured tungsten carbide roller to a honing machine tool for generating micro cavities. They could achieve similar geometrical features compared to laser honing much faster and with significantly less investments and complexity, Fig. 27.

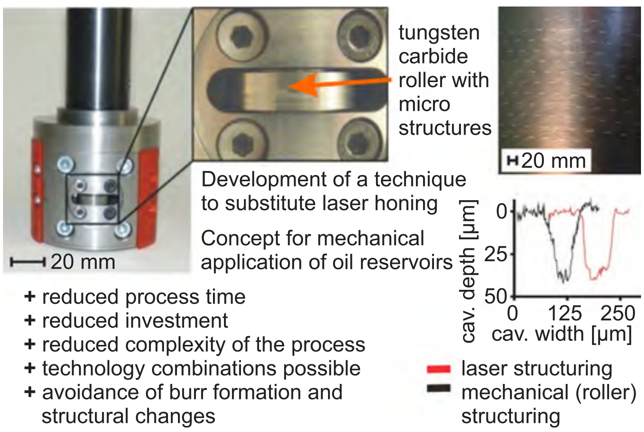

Fig. 27. Micro structuring of cylinder liners by rolling (own work).

3.3. Forming processes

Forming processes are efficient in mass production of multiscale structures. Fabrication of molds is one of the key factors for forming processes. The micro imprinting method using a diamond-coated microneedle permits a single-step production of multilevel three-dimensional surface architectures in a mechanically durable nickel mold. The mold structures can be replicated on polymer surfaces by means of mass-producible replication techniques such as injection molding. Fig. 28 shows SEM images of hierarchical multiscale structures on polypropylene [77]. Similarly, a pyramidal nanoindenter with different revolving trajectories provided by a piezo stage was used to create microstructures on aluminum alloy. Experimental results showed that the revolving scratches could reduce cutting forces and burr formation [177].

By means of hot microcoining, hemispherical structures with varying pocket depths and area densities were produced on stainless steel blanks to produce micro lubrication pockets [134]. Finite element models were also developed to study the steps of the hot microcoining process: heating, cutting, and coining of micro lubrication pockets [152].

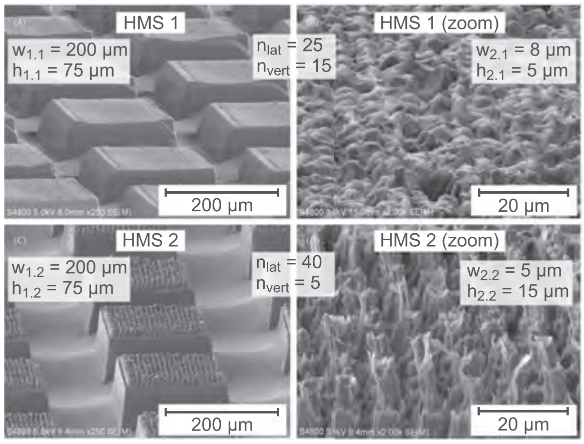

Fig. 28. SEM images of hierarchical multiscale structures on polypropylene surface [77].

A microforming method was used to generate microchannels on the surface of thin sheet metal through a combination of rolling and indentation actions. The deformation based surface texturing is significantly faster and less expensive than etching, machining or laser texturing [210]. For high-rate generation of surface textures, an electrically-assisted microrolling system, featured by using a high-density electric current to soften the workpiece primarily through Joule heating, was proposed [188]. An incremental rolling process was developed to produce riblet structures for viscous drag reduction on fans, compressors and turbine blades. As a metal-forming process, incremental rolling holds many decisive advantages compared to those processes involving material removal or deposition. These advantages include direct structuring of a component, increase in hardness by means of strain hardening, positive grain flow within the rim zone, and compressive residual stresses in the notch groove, through which the fatigue strength of the part is expected to increase. Furthermore, it was shown that the geometry created with rolling processes matches the ideal riblet geometry well [86], as shown in Fig. 29.

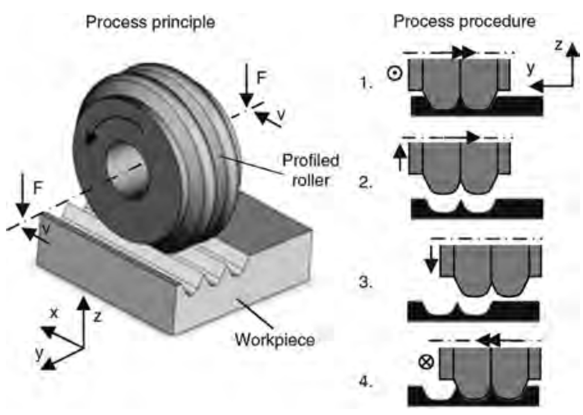

Fig. 29. Principle of incremental rolling for producing defined riblet structures [86].

Compared with traditional manufacturing processes, roll-to-roll (R2R) embossing is an advanced continuous manufacturing method to produce large-volume high-quality micro/nano surface structures on flexible film substrates at significantly lower cost and higher throughput. The R2R has already been used for mass production of brightness enhancement film in the backlight modules of liquid crystal displays (LCDs), and large-area linear Fresnel lens polymer film for solar concentration [207].

3.4. Beam-based processes

3.4.1. Laser beam machining

Laser might be the most flexible tool for multiscale structures patterning. Laser ablation, multi-beam interference and laser-induced periodic surface structures (LIPSS) are major approaches to create the structures.

Laser ablation uses high-intensity lasers to incrementally ablate the substrate materials to create the desired features with typical sizes on the order of 100 nm to 10 μm. For example, nanosecond laser beam machining has been used to manufacture superhydrophobic structures on 316 L stainless steel for biomedical implants and surgical instruments [16].

However, it is difficult for laser ablation to machine materials with high reflectivity or low absorptivity. To overcome the limitation, laser induced plasma micromachining (LIPMM) was developed to create plasma in a liquid dielectric medium above the submerged workpiece to remove material by thermo-mechanical interaction between the plasma and workpiece. Significant enhancements of the basic LIPMM process could be achieved by optical and magnetic manipulation of plasma [188].

A conventional spot-focused laser ablation process is extremely slow for large-area texturing. High efficient techniques include line-focus based laser, multi-laser interference and diffraction-based laser micromachining. Conventional two-beam interference requires the precise alignment of multiple optical elements such as beam splitters, mirrors and focusing lenses along the beam path. Alternatively, a Fresnel biprism was used to split a collimated laser beam into two symmetrical halves and causes them to interfere at a very shallow angle. The biprism interference requires fewer optical elements, lesser optical losses and shorter working distance, and the pattern periodicity is a function of only the biprism side-angle. Biprism can be developed into a highly efficient and feasible option for mass production of micropatterns over large areas [136].

In order to investigate the anisotropic spreading behavior of oil on a periodic structure, multiscale channel-like grooves were produced by combining direct laser interference patterning and microcoining on stainless steel. The produced surface showing the largest anisotropic spreading behavior was due to stronger pinning and increased capillary forces [133].

Ultrashort pulse (picosecond or femtosecond) laser irradiation can significantly decrease the thickness of heat-affected zones. By means of femtosecond laser irradiations at sub-MHz repetition rates, highly regular sub-micrometer LIPSS can be rapidly formed on both metals (Ti, Mo, and steel alloy) and non-metallic surfaces (silicon). The physical mechanisms governing LIPSS regularity on metals are linked with the decay length (i.e. the mean free path) of the excited surface electromagnetic waves (SEWs). As shown in Fig. 30, the mechanisms of LIPSS formation on silicon are considered as the interference of incident laser beam with a scattered SEW, thus resulting in periodic absorption of laser energy [55,56].

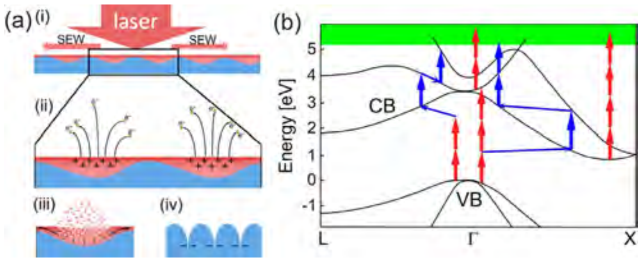

Fig. 30. Schematics of LIPSS formation mechanism on silicon (a) and laser-induced electron excitation (b) [56].

A quasi-uniform distribution of LIPSS on Ti6Al4V titanium alloy substrates can be achieved by a femtosecond Yb fiber laser. The fabricated LIPSS allows to improve adhesive bonding strength with epoxy resin and has the potential to improve the durability of the joints against accelerated aging [135]. Using a Yb-fiber femtosecond laser, homogeneous LIPSS was generated on both aluminum and copper pure metals and stainless steel alloys. In particular, on aluminum the surface morphology results in very high contact angles. LIPSS treatment can be selectively applied to control the interaction with liquids over indefinitely large areas [124]. Using controlled laser fluence and specific defocus position, nanoscale LIPSS formation on a steel mold surface by picosecond laser irradiation was achieved. Plastic forming experiments demonstrated that a steel surface with LIPSS significantly reduced the mold releasing force [88]. Laser texturing has been used to improve the cutting performance of cutting tools [171] and fabricating replication masters for large-scale production of superhydrophobic surfaces on polydimethylsiloxane (PDMS) [103].

As shown in Fig. 31, a triple-level hierarchical periodic surface structure was generated on Ti-6Al-4 V alloy by combining two laser microstructuring techniques with two different pulse durations: nanosecond direct laser writing (DLW) and direct laser interference patterning (DLIP). Contact angle measurements verified a hydrophobic behavior for the hierarchical structures [76].

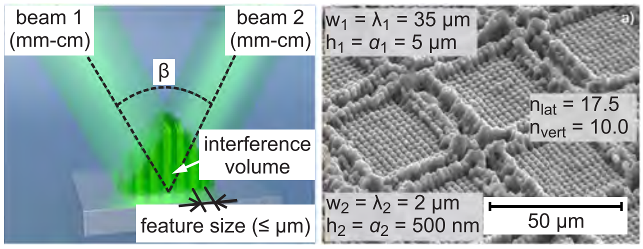

Fig. 31. Schematic for two-beam laser interference patterning [76].

3.4.2. Focused ion beam direct writing

Focused ion beam (FIB) technology is a commonly used technique in the fabrication of micro-/nanostructures [201]. FIB has unique advantages such as high resolution, maskless processing and rapid prototyping. Using FIB, direct writing on Cr thin film was developed to fabricate a nano-photomask with 32 nm line width, which is a single-step process and is cheaper and faster than the traditional lithography process [46]. FIB was also used to pattern nanostructures on Si substrates for developing substrates for surface-enhanced Raman scattering (SERS) [52]. Motivated by the emerging needs for micro-/nanometrology, the fabrication of calibration standards for micro/nano measurement instruments plays a key role in dimensional metrology. FIB has been employed to fabricate the star structures with continuous-variation spoke width for calibration of different precision measurement instruments [174]. FIB milling has also been applied in the fabrication of micro tools as shown in Fig. 32. Periodic nanostructures, diffractive optical elements (DOE) and sinusoidal modulation templates can be fabricated using these tools with a nanometric surface finish [148,176,202].

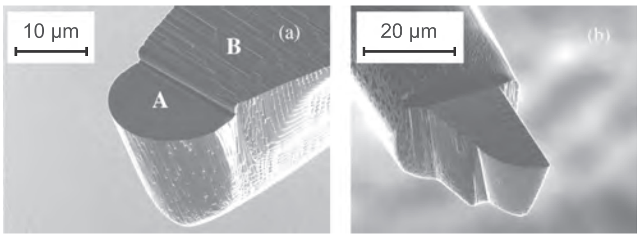

Fig. 32. SEM images of the FIB fabricated micro tools [176].

FIB is also useable for additive (implantation and deposition) processes. FIB implantation (FIBI) has been used in fabrication of nanostructures and nanodevices in which the FIBI layers can be used as the etching mask for subsequent wet etching. A method combining FIBI with subsequent FIB XeF_2 gas-assisted etching (FIB-GAE) was developed to fabricate various micro/ nanostructures on a Si (1 0 0) substrate. The combined process shows several advantages such as high efficiency, flexible and high precision [175].

3.5. Electro discharge and electro chemical machining

As a texturing method possible for mass production, electrical discharge machining (EDM) has been used to texture aluminum sheets to generate stochastic patterns of isolated pocket structures [211]. As shown in Fig. 33, micromilling and die-sinking EDM were combined to manufacture stainless steel inserts with protruding inverted microfluidic patterns.

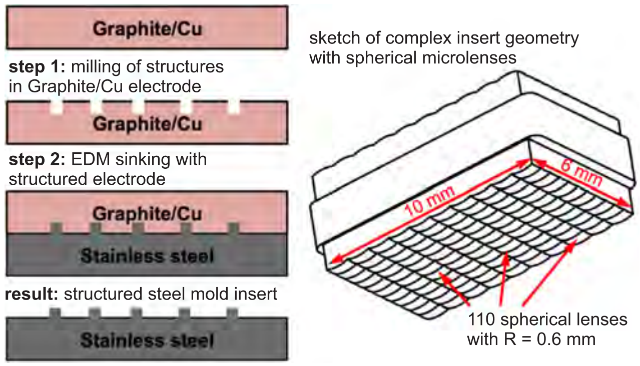

Fig. 33. Procedure for hybrid method combining micro milling of structured Graphite/Cu dies and applying these for EDM sinking in steel (left) and geometrical model of lens array (right) [198].

In a die-sinking EDM process, microfluidic patterns are milled on a graphite/copper electrode; then a thermal erosion process takes place between the tool and workpiece under a controlled electric spark, which has the effect of eroding the workpiece to form a replica of the electrode on a stainless workpiece. This process offers force-free machining independently from the mechanical properties of the processed material and allows batch production of microdies and molds for injection molding and hot embossing. However, electrode wear is significant for machining stainless steel [198].

Büttner, Roth and Wegener applied wire EDM and multiple die-sinking EDM to generate grooves with a width of 31 μm and pillars (Fig. 34) with 84 μm edge length and a depth/height of 220 μm [15].

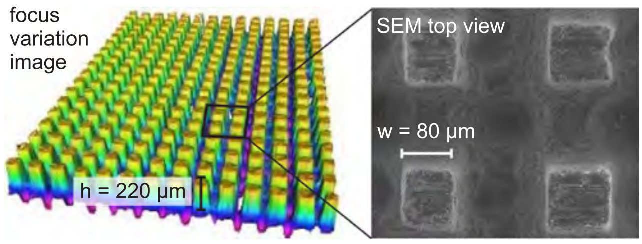

Fig. 34. Micro pillars generated by multiple die-sinking EDM [15].

It is also noteworthy that the material removal rate of EDM processes is higher for porous materials than for solid materials as found by Zou et al. [217]. This could potentially be relevant when manufacturing structured surfaces with heat absorbing, heat exchanging, catalytic or biochemical functionality.

Micro EDM milling is another variant of electro discharge machining that is particularly suitable for generating high aspect ratio microstructures. In a first step, a thin and long EDM tool is generated by using a sacrificial electrode in the shape of a block, a rotating disk or a guided wire. This tool can then be used as an electrode itself to generate micro slots or surface patterns [102]. Another example for high aspect ratio structures are the hexagonal micro electrode arrays produced by Chen et al. by micro reciprocated wire EDM [21].

One of the most critical challenges of micro EDM milling is the progressive wear of the electrode which ultimately affects the accuracy of the machined structures. By using tubular electrodes and a novel compensation algorithm, Pei et al. were able to generate micrometer sized grooves with square or circular geometry with a relative error of 0.3% to 1.2% in groove length and 0.8% to 1% in groove depth [128].

Wang, Qian et al. applied in-situ process monitoring and adaptive control to generate three dimensional sub-millimeter sized cavities with spherical, conic and pyramidal shape [163].

While EDM milling typically is utilized with a liquid dielectric, Uhlmann and Perfilov presented an approach for manufacturing microstructures by dry EDM [161] [Fig. 35]. They utilized 0.2 mm diameter electrodes at n = 280,000 min^{-1} rotation speed in combination with compressed air at 50 bar to generate various protrusions with 100 μm to 600 μm lateral size.

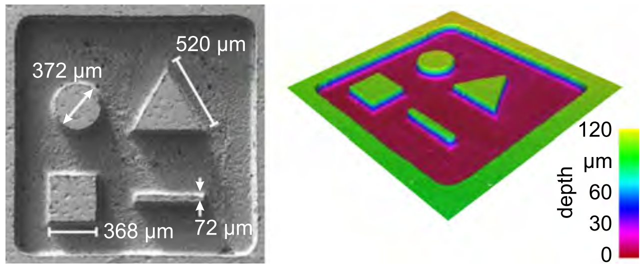

Fig. 35. Features machined by dry micro EDM [161].

By using EDM processes, it is also possible to manufacture hierarchical structures, such as demonstrated by He et al. [65]. In their study, micro- and nanostructures with different surface energy were generated to obtain corrosion-resistant and anti-fouling surfaces.

Zeng et al. used micro EDM milling and electrochemical machining (ECM) for generating square cavities with 0.5 mm lateral size and 0.2 mm depth [191]. They investigated the impact of machining voltage, electrode feed rate, machining gap on the performance of the processes. With an optimized set of parameters, they were able to achieve a surface roughness of 0.707 μm by EDM, which was further reduced to 0.143 μm by ECM, while the mechanical properties of the surface were improved simultaneously.

In solar cell technology, surface texturing is essential for reducing the reflectance of cell surfaces and increasing their efficiency. Photo-assisted electrochemical etching (PAECE) was developed to fabricate a hybrid structure comprising a reversed pyramid structure and a high aspect ratio macro-pore on the silicon wafer surface. [72]. A similar approach is high-density plasma etching of hierarchical anti-reflective structures [24].

3.6. Lithography processes

3.6.1. Direct patterning by lithography

Photolithography is a well-established process in the fabrication of complicated multiscale structures. However, a curved substrate is hard to process by conventional photolithography. The optical soft lithography technique using a flexible PDMS photomask, which can be fit uniformly on a curved substrate, was developed to transfer micro patterns onto a curved substrate [127]. Multiscale hierarchical structures inspired by moth's compound eyes offer multifunctional properties in optoelectronic devices. The roll-to-roll ultraviolet nanoimprint lithography (R2R UV-NIL) technique was used to fabricate the multiscale compound eyes arrays on PET substrates [129], see Fig. 36.

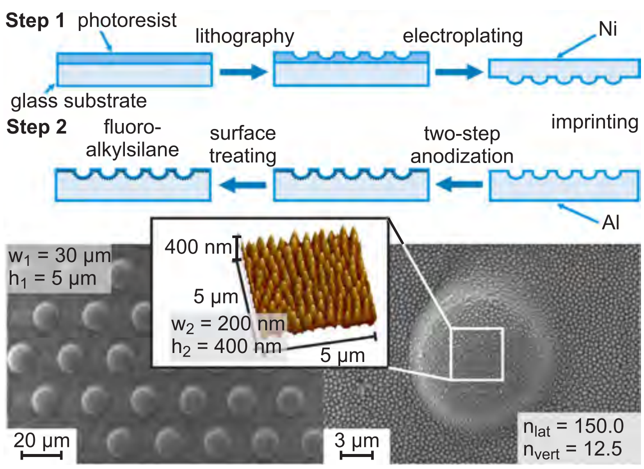

Fig. 36. UV nanoimprinting lithography process and multiscale compound eye array [129].

Multibeam interference lithography has been shown to be a fast, simple, and versatile approach to the creation of periodic porous microstructures. When two or more optical waves are present simultaneously in the same region of space, the waves interfere and generate periodic variations in intensity and polarization, which can be transferred into a conventional photoresist film (up to 100 μm thick) to yield periodic lithographic structures with submicron resolution [183]. However, as long as propagation light is used, fabrication of fine structures less than half of wavelength is difficult. The processing resolution can be improved by using evanescent wave instead of propagation light [114].

Compared with conventional ultra-violet (UV) lithography, synchrotron-based hard X-ray lithography offers advantages for fabricating thick patterns with smooth sidewall roughness owing to the high transmittance and straightness properties of X-rays. A hard X-ray lithography process was proposed for fabricating complicated multiscale structures that include submicron patterns [84]. The procedure employs a combination of typical UV-based X-ray masks with micron patterns and metal deposited X-ray masks with sub-micron patterns. Contact-based nanoimprint lithography (NIL) techniques, such as thermal and UV nanoimprint are considered the next generation lithography. In order to fabricate nano/microscale hybrid structures, the roll-typed liquid transfer imprint lithography (R-LTIL) system and process were developed and hybrid patterns were clearly fabricated [97].

Recently, a technique called nonlinear laser lithography (NLL) has been introduced which permits mass production of highly uniform nanostructures on large surface areas with an elevated production rate. This technique is based on the use of a high repetition rate, well-focused femtosecond laser with pulse energy in the order of nanojoules [123].

Complex optical microstructures can be fabricated by using lithographic methods such as inclined immersion lithography [19], and lithography can be further improved by chemical etching. For example, photolithography and chemical etching methods are combined to make microdimple patterns on hardened steel material [63]. As nanoimprint lithography is one of the most promising technologies for nanoscale patterning, and plasma etching processes are effective in inducing roughening without affecting the bulk properties of the polymers, the combination of these two technologies allows the creation of hierarchical structures on polymeric films [40].

Flash foam (FF), also called photosensitive seal, is a type of ultra-micro bubble material. The most unique characteristic of FF is that when it is exposed to an intense burst of light, its microporous surface will be sealed. When a mask on top of the flash foam is exposed, the mask pattern will be transferred to the flash foam to create a flash foam stamp (FFS). If ink is stored in the porous FF, the mask pattern will be stamped onto paper through the unsealed surface area. Thus, flash foam stamps are more convenient than traditional hard stamps due to their high resolution and inkpad-free stamping process. A soft lithography method called flash foam stamp lithography (FFSL) was developed and used for micro casting and soft lithography [64].

Multiscale surface structures are common in nature. The seta on the toe pad of geckos' branches into a dense array of microscale cylindrical structures with nanoscale tips, which generate large adhesive and shear forces when they come into contact with a surface. The microscale patterns can be defined using conventional photolithography followed by dry etching, while the nanoscale tips are produced using colloidal lithography in conjunction with dry etching. As shown in Fig. 37, the fabricated hierarchical structures are considerably hydrophobic.

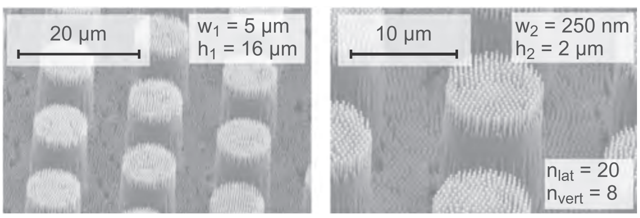

Fig. 37. SEM photographs of hierarchical structures featuring microscale cylinders with nanoscale tips [78].

The strong adhesion properties of a gecko foot can be attributed to van der Waals forces produced by the nano-structures on the spatula [78]. Moreover, the *Attacus atlas* moth eye is characterized by non-planar, 3D microlens arrays with a subwavelength antireflective nanostructure. A soft lithographic technique was used to fabricate multiscale topographically faithful molds, which is used to replicate the original eye surface with nanoscale fidelity [87].

Maskless grayscale lithography technique is a promising technique for directly fabrication 3D microstructure without hard masks. Multilayered patterns are superposed on a photoresist layer by layer so as to realize a 3D profile. After a development with an appropriate time, 3D profile of photoresist corresponding to the profile of the UV dose is obtained. The patterns could be transferred into silicon substrates with reactive ion etching (RIE). Maskless grayscale lithography is especially advantageous for developing MEMS devices [158]. Microlens arrays can be fabricated by using gray-scale photolithography. However, the grayscale photomask costs are extremely high. Therefore, a diffuser lithography was proposed to fabricate both spherical and aspherical microlens arrays. Microlens arrays were fabricated by the combination of diffuser photolithography and molding techniques, as shown in Fig. 38 [80].

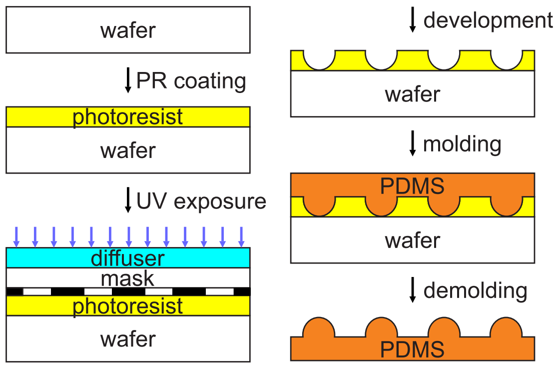

Fig. 38. Combining diffuser photolithography and molding for making microlens arrays, according to [80].

Nano-porous anodic alumina (nano-PAA) film is a very attractive material due to its controllable nanoscale geometry, including the thickness of the film, the pore diameter and inter pore distances. Hybrid micro/nano-structural surfaces were prepared on porous anodic alumina using the ultraviolet lithography method followed by the two-step anodizing method. Based on a combined method of surface structuring (Fig. 39), the controllable hydrophilicity over a large area could be attained. By the same method, the super-hydrophilic surfaces could be made as well [164].

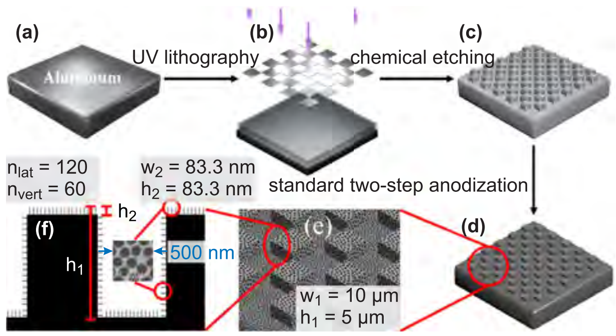

Fig. 39. Ultraviolet lithography followed by two-step anodizing for multiscale structures with super-hydrophilicity [164].

Laser lithographic approaches have also been attempted for fabrication of structured surfaces, such as laser direct-write lithography and holographic lithography. Holographic lithography employs spatial overlapping and optical interference of multiple coherent beams to generate 2D or 3D periodic optical patterns that are recorded in photosensitive materials. Phase masks enable a robust type of holographic lithography that employs phase gratings to produce multiple diffraction beams and spatially combine them to form 2D and 3D periodic interference patterns [186]. Laser scanning holographic interference lithography was developed to form both micro- and nanostructures in a single exposure step [187].

3.7. Chemically assisted manufacturing processes

Liquid and gas chemical agents are usually used for assisting mechanical manufacturing processes to improve the material removal rate and/or surface integrity. Chemical reactions among solids has also be attempted for this purpose. For example, carbon diffusion reaction between transitions metals and carbon have been used for machining diamond [179]. Though diamond is stable at room temperature, it has high affinity with specific transition metals (Ni, Fe, Ti, etc.) at a high temperature. The transition metals can absorb carbon atoms from a diamond surface. When a structured transition metal mold is pressed against diamond under high temperature and pressure, carbon atoms are directly absorbed by the mold, enabling rapid machining.

3.7.1. Etching techniques

Etching may, for instance, be applied to generate structures on the {210}-plane of single-crystal ammonium perchlorate. In the study of Lucca et al., this was utilized to generate defined 2 μm by 5 μm rectangular pits with a depth of 50 nm and an areal density of 3-4 $\cdot$ 10^6 cm^{-2} for nanoindentation analysis [110].

In order to fabricate superhydrophobic surfaces on titanium substrates, sandblasting, acid-etching, and anodic oxidation were used to generate hierarchically structured surfaces with micro valleys and nanotubes. Afterwards, fluoroalkylsilane was used to reduce the surface energy [131]. The results showed that the micro-nano hierarchical surface was hydrophilic. However, after modification by fluoroalkylsilane, the surface converted from hydrophilic to superhydrophobic. To fabricate aluminum superhydrophobic surfaces, a simple method was used to generate microterrace nanoleaf hierarchical structures. Microscaled rough surfaces were produced by a simple etching method using Beck's etchant while nanoscale structures were achieved by dipping in sodium chloride solution [85], as shown in Fig. 40.

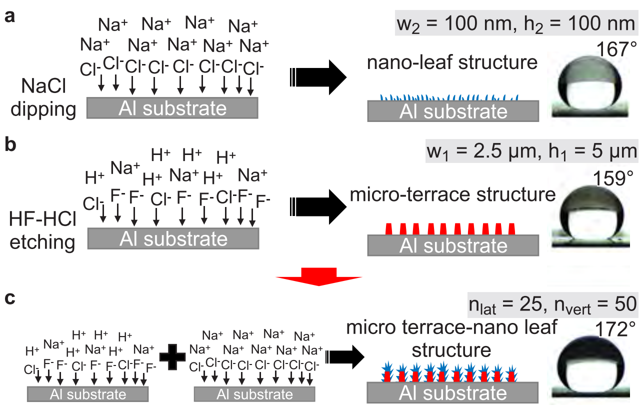

Fig. 40. Schematic illustration of formation of (a) nano-leafs by dipping in NaCl solution, (b) micro terraces by etching in Beck's etchant, and (c) microterrace nanoleaf hierarchical structures by etching and subsequent dipping in NaCl solution [85].

A facile approach combining template and etching methods together was applied to fabricate regular hierarchical multiscale structures on a copper foil using the back surface of fresh bamboo leaf as the original template [189]. After the hierarchical multiscale structure was constructed on the copper foil surface, the water contact angle of the copper foil surface increased from 64° to 131.1° Then the copper foil with hierarchical structure was modified by stearic acid, and the copper foil surface with hierarchical multiscale structure showed superhydrophobic property with a contact angle of 160.0° This method opens a new way for the transfer of hierarchical micro-, submicro-, and nanostructures of natural species onto metal surfaces. Fabrication of superhydrophobic textured steel surface for anti-corrosion and tribological properties was also reported [194]. Micro/nano multiscale structures were made by KOH wet etching, improved DRIE process and gold sputtering [209].

3.7.2. Chemical synthesis

A new printing strategy, namely matrix-assisted catalytic printing (MACP), was proposed for versatile fabrication of metal patterns (Cu, Ag, Ni, Au) with feature sizes spanning from nanometer to meter scales. The key innovation of MACP, as shown in Fig. 41, is the use of matrixes (both delivering and receiving) to carry and immobilize the catalysts on the substrates, so that subsequent electroless deposition can be carried out site-selectively to yield highly conductive metal conductors [60].

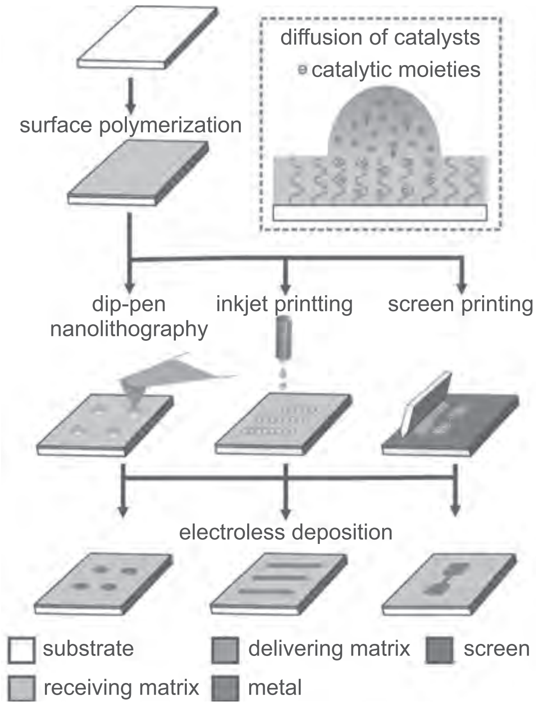

Fig. 41. Schematic of matrix-assisted catalytic printing (MACP) process used in dip-pen nanolithography, inkjet printing, and screen printing. [60].

Catalytic chemical vapor deposition (CCVD) was used for the synthesis of hierarchically structured nanocomposites, which represents carbon microfibers covered with a layer of carbon nanomaterials [94]. The way of catalyst deposition affects both the yield and structure of the carbon nanofibers grown on the microfiber surface.

Nanomaterials have attracted considerable attention. Various studies of nanogenerators (NGs) based on ZnO nanowires (NWs) by chemical growth and spin coating were reported [23]. In addition, ionotropic gelation and ceramic tapecasting were used for micro and sub-micro patterning [8]. Self-assembled nanorods from chemical synthesis was used for hierarchical nanostructures [18]. Low dimensional SnO_2 structures exhibit brilliant gas-sensing properties. SnO_2 hierarchical structures assembled by either nanoneedles or nanosheets were synthesized through hydrothermal method. The existence of PVP (polyvinyl pyrolidone) can tailor the morphologies and control the sizes of the blocking units [172]. Ag nanowire/ZnO nanobush hybrid structures have been synthesized by a combination of polyol method and low-temperature solution method. The photocatalytic activity of Ag/ZnO hybrid nanostructures was greatly improved compared to pure ZnO nanostructures [153]. Nanoflake and nanowire hybrid structures may be synthesized by plasma-enhanced hot filament CVD and can potentially be applied for next generation optoelectronic modulators and filters [162].

3.8. Other processes and process combinations

Numerous innovative processes for generating multiscale structured surfaces are currently under research and development which do not fit in traditional boundaries of a singular technology. This includes specialized additive machining technologies [122], processes using (self-) assembly of smaller building blocks or sequences combining multiple process. Especially replication technologies fall under the latter category, as generally a combination of multiple processes if required for mold machining and replication, see [47,62,138].

3.8.1. Replication processes for hierarchical structures

For replication processes, the transferability of the structure' shape from the mold to the replica is a general concern when setting up the required process, as numerous factors affect the molding conditions. Generally, it must be assured that a proper demolding of hierarchical structures is possible. Furthermore, the structuring fidelity, e.g. complete filling of the cavity and only minimal deformation of the structures, has to be assured by the molding process. This is especially important for optical applications, since incomplete filling or rounding of prismatic structures affects the imaging quality of the molded structures [113]. In this context, Zhou et al. have investigated the stresses occurring in ultraprecision glass pressing of microgrooves and found these decrease with increasing mold temperature and increase proportionally to the press velocity [212]. Form errors mainly occur at groove valleys of the molded part as the sides of the microgrooves are deformed during molding. Thus, it is extremely challenging to replicate fine and delicate structures. The same is also true for high aspect ratio structures, such as deep channels in microfluidic chips for example, for which a complete filling is only achieved under the right molding conditions [193]. A technique commonly used for high fidelity replication of microstructures is the variothermal molding, in which the melt is not heated to a specific target temperature but follows a heating profile specific to the part and processing conditions. With this, it is possible to achieve a high fidelity filling of micro pattern, including the replication of sharp corners, as shown by Zhang et al. [199,200].

By purposely deforming the mold prior or during molding, hierarchical structures may be generated. Bae, Jeong and Kim apply this technique by first fabricating a polyurethane acrylate (PUA) master mold with hexagonal arrays of nanopillars using photolithography and reactive ion etching [5]. The master is then pressed onto an ultraviolet/ozone-cured polydemethylsiloxane (PDMS) sheet, cured by UV light, and peeled off from the master mold. This PDMS is then subjected to uniaxial strain to cause wrinkling of the flexible sheet. In the last step, a PUA replicate is obtained from the PDMS by molding and curing. This final product is a multiscale substrate that features the large-scale structuring of the wrinkles overlaid by the small scale nanopillars (Fig. 42).

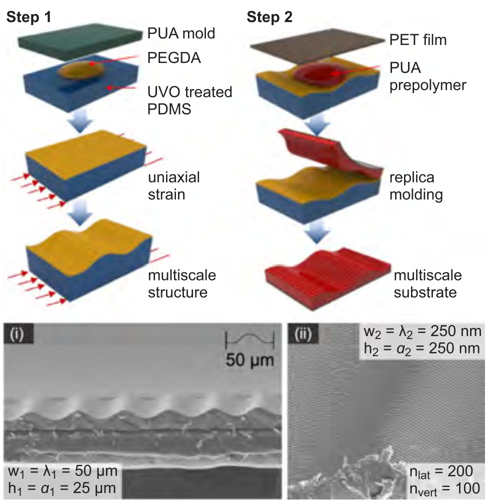

Fig. 42. Multi-step replication of hierarchical structures: fabricating and deforming a structured PDMS sheet (step 1) and replicating a multiscale substrate from this (step 2), adapted with permission from [5].

The manufacture of structures on multiple scales is also possible by combining focused ion beam (FIB) sputtering techniques, incremental forming and molding. As FIB sputtering is only effective on a small scale, it was used by Matsumura et al. to generate a micro structured stamping tool [115]. This was then used to pattern a metal substrate in an incremental forming procedure. By varying the pitch of the stamping procedure, a large scale pattern of small scale micro structures is generated.

Another method called sacrificial layer mediated nanoimprinting, which involves nanoimprinting aided by a sacrificial layer, was developed by Raut et al. [130]. The fabricated arrays, as shown in Fig. 43, exhibits excellent pattern uniformity over the entire patterned area.

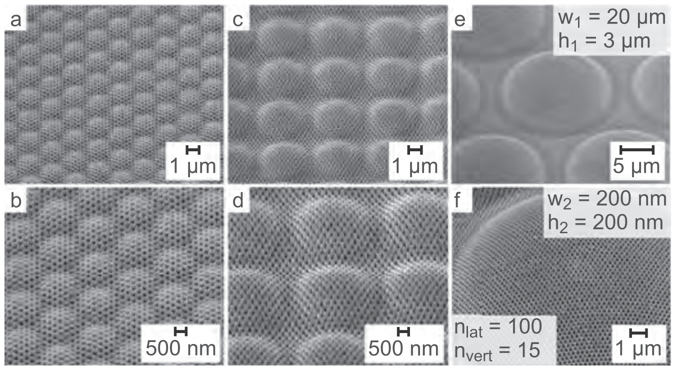

Fig. 43. SEM images of multiscale ommatidial arrays [130].

These arrays exhibit multifunctional properties such as broadband and omnidirectional antireflection as well as superhydrophobic and antifogging characteristics, which has potential applications in image sensors, solar cells, LEDs, and so on.

3.8.2. Self-assembly

The self-assembly of hierarchical structures from inorganic and biological materials is of great interest for the design of novel bio-activated devices. The primary challenge with this technology is to effectively control the material interfaces in a way that deterministic and functional patterns are formed. While in some cases, these synthesized structures are used to cover a technical surface, many applications target the generation of hierarchically structured particles, i.e. micrometer- or nanometer-sized elements that have a hierarchical surface structure. Due to the relevance of the topic in bio-technical applications, a short overview of current developments will be given here.

For example, Hnilova et al. demonstrated a versatile and flexible assembly technique which they use to generate layers of proteins connected with gold nanoparticles bottom-up [69]. By combining this with lithography and specialized peptide tags, the special assembly of proteins becomes well controllable. Hu et al. were able to coat 10 to 270 nm thick nanoscale gold (Au) clusters on polystyrene (PS) spheres with a diameter of 151 to 360 nm by utilizing the self-assembly of the PS spheres, Au coating thickness regulation and FIB nano-patterning [70]. This may be used for surface-enhanced Raman spectroscopy in advanced biotechnical sensors, e.g. for cancer screening and detection.

3.8.3. Additive manufacturing

With the advancement of additive machining processes, the generation of structured surfaces using this technology gains more and more importance. Due to geometry being formed by different layers of fused material, the surface obtained from these processes is (un)intentionally structured out-of-the-box [2], making the controlled generation of a specific microstructure or surface texture a challenging task. Nevertheless, significant progress has been made to generate defined micro geometries using additive technologies. Zhang, Qu et al. have used dynamic optical projection stereolithography (DOPsL) to fabricate complex 3D shapes (Fig. 44) in soft, degradable biomaterials [192].

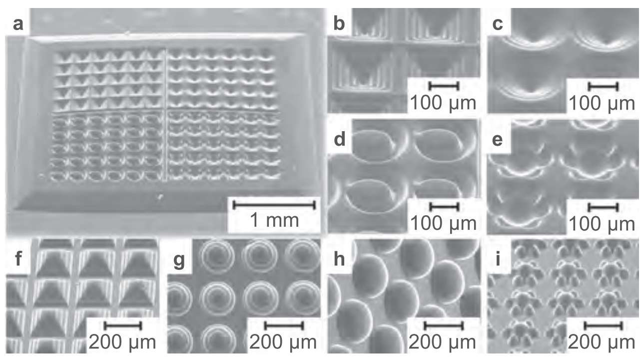

Fig. 44. Microstructures generated by DOPsL [192].

Guo, Yu et al. utilized a technique called matrix-assisted catalytic printing (MACP), in which an 'ink' consisting of deionized water, inorganic catalytic salt and a delivering matrix polymer is printed on a substrate that is modified with a thin polymer layer as the receiving matrix [60]. This forms a catalyst pattern on the surface that allows the subsequent electroless deposition of metal, e.g. for generating copper conductors. They demonstrate the applicability of several printing techniques to generate structures of varying complexity and scale. More recently, Davoudinejad et al. showed the direct manufacture of hydrophobic surface structures using photopolymerization techniques [26].

With bioprinting technologies it is even possible to additively manufacture biomasks for facial skin reconstruction [139]. Relating the porosity of the printed mask to the size of the facial features indicates that this has to be considered as a multiscale structured surface.

4. Applicability of manufacturing processes across scales

The applicability of manufacturing processes or a process sequence across different orders of magnitude is the basis for being able to generate multiscale structured surfaces. While the previous section has presented manufacturing processes from various technological fields and indicated exemplary structures that can be produced by them, this chapter will focus on the specific potentials and limitations of the technologies to generate multiscale structures. The capabilities of singular processes will be assessed first and thereafter possibilities to establish process chains with the available technologies will be discussed.

Table 4 summarizes examples of multiscale structured surfaces generated by various researchers and their potential application. It also states the respective lateral and vertical extent of the base structure and substructures and shows the calculated multiscality values according to the definition proposed in this keynote paper.

Moreover, a graphical representation of the lateral and vertical dimensions achievable by the processes reviewed in this paper is also shown at the end of Section 4, in Fig. 46. This figure has been automatically derived from all evaluated literature items by first grouping the processes by chapter and then drawing a polygon for each group representing the convex hull of the values for the lateral and vertical extents of the associated processes.

4.1. Scalability of singular processes to different scales

Having a single process available to generate structured surfaces across different scales is the preferable option in most cases, insofar as this obviously eliminates the necessity for an additional part fixing and alignment and handling between processing steps. However, only few processes can generate multiscale structured surfaces without the need for additional processing steps or technologies. In general, most machining technologies are can be considered single step processes, as well as some etching techniques and chemical synthesis processes.

Minimal and maximal structure sizes as well as structure complexity are, however, limited by a couple of factors determined by the utilized process. Depending on whether the technology focuses on a top-down (material removal, forming) or bottom-up (additive, synthesis) approach, either the minimal achievable structure size or the maximal structure size limit the manufacturing capability. In all machining processes, for instance, the smallest machinable structure size is the result of the positioning accuracy of the machine tool, minimum feature size that can be realized for the removal tool and the flexibility of how this tool can be guided and aligned in 3D-space. For

Table 4
Hierarchical structures and calculated multiscality values (sorted by lateral and vertical multiscality).

	Authors	Application	process(es)	Structure 1 (base)			Structure 2 (sub)			Multiscality	
				type	lateral	vertical	type	lateral	vertical	n_{lat}	n_{vert}
single techn.	Kim et al. [85]	surface wetting	etching	µ-terrace	w ≈ 2.5 µm	h ≈ 5 µm	nano leaf	w ≈ 100 nm	h ≈ 100 nm	25	50
	Huovinen et al. [77]	bio-inspired	forming	plateau	w ≈ 200 µm	h ≈ 75 µm	micropit	Ø ≈ 8 µm	h ≈ 5 µm	25	15
	Guo et al. [59]	surface wetting	EVC cutting	groove	w = 100 µm	h = 20 µm	texture	λ = 5.5 µm	a = 500 nm	18	40
	Xu et al. [173]	biomedical	EVC milling	groove	w ≈ 140 µm	h ≈ 3.5 µm	texture	w ≈ 8 µm	h ≈ 1.75 µm	17.5	2
	To, Zhu et al. [157,216]	optical	EFCS milling	microlens	Ø = 240 µm	h = 1.2 µm	dimple	w = 20 µm	h = 445 nm	12	2.7
	Cao et al. [18]	tribological	chem. synthesis	sphere	Ø ≈ 1 µm	h ≈ 1 µm	spike	w ≈ 100 nm	h ≈ 500 nm	10	2
	Ta et al. [153]	photocatalysm	chem. synthesis	nanowire	Ø ≈ 94 nm	h ≈ 1 µm	nanobushes	Ø ≈ 10 nm	h ≈ 95 nm	9.4	10.5
	Cheung et al. [22]	optical	STS turning	sinusoidal	λ = 5 mm	a = 80 µm	microlens	p = 2 mm	h = 50 µm	2.5	1.6
multi-step / multi physics	Lee et al. [97]	optical	R-LTIL + replication	microlens	Ø = 80 µm	h = 10 µm	pit/dimple	Ø = 350 nm	h = 250 nm	229	40
	Bae et al. [5]	cell culturing	PDMS molding + forming	sinusoidal	λ = 50 µm	a = 25 µm	grooves	w = 250 nm	h = 250 nm	200	100
	Ko et al. [87]	optical	lithography + molding	microlens	w ≈ 30 µm	h ≈ 8 µm	antirefl. pattern	w = 170 nm	h = 200 nm	176	40
	Peng et al. [129]	optical + surface wetting	lithography + electroplating + imprinting	microlens	Ø = 30 µm	h = 5 µm	pillar	Ø = 200 nm	h = 400 nm	150	12.5
	Zhang et al. [209]	optical	photolith. + etching	inverted pyramid	w ≈ 14 µm	h ≈ 14 µm	spikes	w ≈ 100 nm	h ≈ 800 nm	140	17.5
	Wang et al. [164]	surface wetting	lithography + etching	rectangular array	w = 10 µm	h = 5 µm	nanopores	Ø = 83 nm	h ≈ 83 nm	120	60
	Raut et al. [130]	optical + anti-fogging	imprinting + coating	microlens	Ø = 20 µm	h = 3 µm	nano-pattern	λ ≈ 200 nm	a ≈ 200 nm	100	15
	Rosenkranz et al. [133]	surface wetting	micro coining + DLIP	coined grooves	w = 400 µm	h = 40 µm	DLIP grooves	w = 5 µm	h = 1 µm	80	40
	Takayama et al. [154]	structured tools	laser mach. + cutting	V-groove	w = 300 µm	h = 15 µm	groove	w = 5 µm	h = 3 µm	60	5
	Durret et al. [40]	surface wetting	NIL + etching	pillar	Ø ≈ 600 nm	h ≈ 600 nm	spikes	w ≈ 11 nm	h ≈ 11 nm	54	54
	Masui et al. [114]	optical	lithography + film devel.	elliptic lens	w = 13 µm	h = 250 nm	grating	λ = 450 nm	h ≈ 50 nm	29	5
	Jheng et al. [78]	bio-inspired	lithography + etching	pillar	Ø = 15 µm	h = 16 µm	spikes	Ø = 250 nm	h = 2 µm	20	8
	He et al. [64]	not specified	printing + exposure	circular pattern	w ≈ 230 µm	h ≈ 2 µm	square pattern	w ≈ 12 µm	h ≈ 1 µm	20	2
	Huerta-Murillo et al. [76]	surface wetting	DLW + DLIP	microgrid	w ≈ 35 µm	h ≈ 5 µm	LIPSS	w ≈ 2 µm	h ≈ 500 nm	17.5	10
	Chou et al. [24]	optical	lithography + etching	paraboloid	Ø = 800 nm	h = 1 µm	spikes	w ≈ 70 nm	h ≈ 75 nm	11.4	13.3
	Huang et al. [72]	optical	photo-assisted electrochemical etching	inverted pyramid	w = 50 µm	h = 40 µm	bores	Ø = 5 µm	h = 67.1 µm	10	1.68

Ø diameter, *w* width, *h* height/depth, *l* length, *p* pitch, λ spatial frequency, *a* amplitude; *values in italics have been estimated from figures in the reference.*

cutting processes, this entails the sharpness of the cutting edge and the geometric details that can be realized on it while for energy-based processes the minimum diameter of the directed energy beam (laser, UV light), the spot geometry and the intensity profile are relevant. At very small structure sizes in the low nanometer range, material properties also must be factored in, because these affect the surface generation mechanisms in this regime.

Being able to generate very small and geometrically defined structures with cutting processes almost always requires the use of diamond machining technologies, because only these allow for ultra-sharp cutting edges and fine geometric details of the cutting tools. They come, however, with the price of only being able to machine a limited spectrum of materials without catastrophic tool wear and are also limited by very low removal rates [141]. For machining structures of larger size, cutting processes are mainly limited by the extent of the machine's positioning capabilities, i.e. the stroke of the axes, and the permissible loads for the cutting tools. Especially tools with fine geometric features are very fragile and must be operated only with low loads. This results in large-scale structures being typically cut in several layers with a constant undeformed chip thickness.

The structure size and complexity that can be generated with a single cutting process is also closely connected to the machining kinematics (see Fig. 45). For example, turning processes can cover a large-scale ratio in lateral direction, whereas they are limited in the structure's vertical direction by the spindle speed and the dynamics of the infeed axis. This becomes obvious for Fresnel type of structures that typically feature multiscalities of $n_{lat} = 5$, as in [75], to $n_{lat} \geq 20$, see [95,181], in lateral direction, but no variation in structure height ($n_{vert} = 1$).

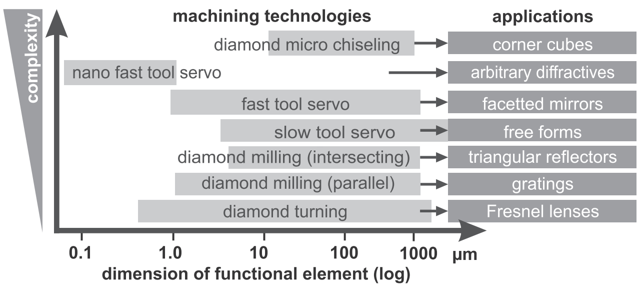

Fig. 45. Selected technologies for generating functional surface structures and related examples, cf. [9,50].

Rotation-based processes, like turning, milling and grinding, are always limited in their structure geometry by the rotation radius, whereas cutting processes with 3D-flexible kinematics, like DMC [11], allow for the generation of structures across a broad size range, potentially allowing for height and lateral size ratio of up to 50. Nevertheless, rotatory process kinematics may also be used in conjunction with other machining parameters (feed, spindle speed) to generate surfaces with subfeatures of a lower size level than the originally machined structure. This typically is used in conventional milling processes and may either result in a surface texture, e.g. as in [6], or geometrically semi-defined elements, such as dimples [117] or pits. While an additional functionality is embedded into the surface in this way, multiscalities are normally only on a very low level in terms of the scale defined for this keynote paper ($n_{lat} = 1–2$; $n_{vert} = 1–2.5$).

If geometrically well-defined structures are to be produced in cutting, the dynamics of the machine axes have to be increased according to the relative cutting speed and feed velocity. While low frequency movements can be handled by the machine axes themselves (Slow Tool Servo, STS), higher dynamics are typically achieved by adding dynamic infeed axes, such as Fast Tool Servos (FTS). An example for STS machining of a multiscale structured surface is the hierarchical microlens array that is analyzed by Cheung et al. in [22]. This sample features 50 μm deep microlenses with a 2 mm spacing on a sinusoidal surface with 5 mm periodicity and 80 μm amplitude. The respective height ratio is $n_{vert} = 1.6$ and the lateral size ratio is $n_{lat} = 2.5$, resulting in an overall medium multiscality according to Table 1. Higher frequency tool actuators (FTS) increase the multiscality only by small factors in vertical and lateral direction, and achieve a high multiscality in vertical rather than in lateral direction, as shown in [214] with $n_{lat} = 3$ (medium) and $n_{vert} = 3.5$ (high). Very high multiscalities are only achieved after further increasing the dynamics of the tool motion, as shown by Guo et al. who machined hydrophobic textures with 500 nm height and 5.5 μm wavelengths on a grooved surface (characteristic height 20 μm, pitch 100 μm) using elliptical vibration cutting [59]. This calculates to multiscalities of $n_{lat} \approx 18$ and $n_{vert} = 40$, i.e. in the range defined as "high". Zhang, Suzuki and Shamoto have shown that it is possible to generate defined surface structures ranging from 2 nm to 1 μm height and from 250 nm to 150 μm periodicity ($n_{lat, vert} = 500–600$) with the same process [195].

More general means to enable multiscale structuring with cutting processes in a single pass is the structuring of the cutting tool itself, whether it is the grinding wheel [27], the milling tool [167] or the turning tool [202]. This, however, required multiple dedicated manufacturing steps to first structure the tool and then structure the workpiece, which will be discussed in the following Section 4.2.

Other singular processes are also capable of generating structures across multiple scales. With forming processes, for example, it is possible to generate hierarchical structures in step-and-repeat processes using structured dies or needle type indenters. Size ratios of $n_{lat} = 25$ and $n_{vert} = 15$ are achievable with such techniques [77] .

Beam-based processes, such as laser beam machining, offer a great extent of flexibility regarding the structure sizes that they are able to create. The size of machinable features ranges from only a few nanometers (e.g. electron or ion beam writing) to several micro- (laser ablation) or even millimeters (laser beam machining). In addition, optical effects, such as interference, may be exploited to generate periodic, nanometer-sized features on the machined surfaces.

Electro discharge machining is especially capable of generating high aspect ratio structures. The minimal structure size of these technologies is limited by the size of the electrode and – as it is vital that the electrode and the workpiece do not get in touch during the process – the gap size that can be reliably set. In general, the generated feature is always larger than the electrode, as the machining principle relies on an electric spark to discharge at the tool-workpiece interface and the induced melting and vaporization of material. In addition, the conditions of the electrode constantly change during the process as a result of wear and therefore need to be controlled with care. In any case, the machining depth can be several times larger than the width of the structure, e.g. 220 μm in depth as compared to 31 μm in width as shown in [15] or even 700 μm in height for 40 μm width as in [21]. The generation of nanoscale structures, e.g. nanopores [65], with EDM, however, can only be achieved by carefully controlling the processing parameters. Nevertheless, the generation of hierarchical structures is possible in this way.

Last but not least, additive machining technologies inherently offer the possibility to generate structures across an extremely wide size scale that is only limited by the smallest achievable structure size at the bottom end (e.g. a few nanometers with stereolithography [192]) and the workspace of the machine on the other end (several millimeters in [192]).

4.2. Multi-step and multi-physics processes

Overall, relying on a single machining technology for the generation of multiscale structured surfaces is somewhat limiting. Thus, sequences of processes are often used to generate hierarchical elements on a surface. This includes the subsequent application similar manufacturing technologies on different scales (multi-step processing, e.g. conventional cutting and diamond machining) or approaches based on entirely different physical principles (multi-physics).

Particularly, the aforementioned lithographic processes belong to the latter category, with the features either being inscribed into a reactive surface using an energy beam and then chemically removed via etching to obtain a structured surface (e.g. photolithography) or with the (nano) structures being directly inscribed into a substrate and then used for replication (e.g. imprinting nanolithography). With such processes, it is possible to generate a variety of nanoscale features on top of microscale structures. Generally these processes are capable of reaching the highest multiscalities of all processes considered in this keynote paper, with values of 30 to 230 in lateral direction and from 10 to 40 in vertical direction being typically achieved, see [97,129,130].

By subsequently applying different working principles, the advantages of each machining technology may be combined in order to generate features in a size range and complexity suitable for the respective technology. Taking hierarchical micro- and nanostructures as an example, it would surely be possible to generate those solely by the application of cutting processes, e.g. by micromilling the larger structures and diamond machining the nanostructures. The smaller the structure size gets, however, the more time is required for the machining procedure, as tool size, feed and stepsize would have to be reduced accordingly. Thus, the economic efficiency of the procedure is severely limited. On the other hand, an etching procedure is able to generate nanoscale surface patterns, as in [85], but the etching rates and even chemical saturation limit the upscaling of this procedure to larger structure sizes. Consequently, the subsequent application of both technologies enables the generation of hierarchical structures with a much higher multiscality than the individual technology would allow. Values of more than 100 in lateral direction and more than 20 in vertical direction are easily achieved (cf. Table 4).

Examples for process combinations that have successfully yielded hierarchical and multiscale structured surfaces and that are seen to be of particular importance for the future manufacturing of functional parts are summarized in the following:

Forming processes to generate large scale structures in combination with laser beam machining to generate finer sub-structures. - *This enables the generation of hierarchical structures with multiscality values of up to* $n_{vert} = 40$ *and* $n_{lat} = 80$ *[133].*

The manufacture of structured cutting edges and the subsequent cutting of hierarchical structures by using them [168]. – *This is seen as a promising approach, because it extends the structuring capability of almost any cutting process to multiscale structures.*

The combination of mold making and forming processes for the replication of multiscale structured surfaces. Either multiscale molds can be directly generated by forming [77] or previously molded parts can be (de-)formed to generate novel surface structures [5]. – *This combination is favorable, because both processes are suitable for mass production due to their generative nature,* i.e. *being able to produce a multitude of surface structures in a single step.*

Lithographic techniques in combination with replication processes, e.g. coining or imprinting. – *(Photo-)lithographic processes are particularly suitable for generating lateral structures in the nanometer range, to compensate for the limited size range in vertical directions, they are best utilized in combination with other processing techniques to generate multiscale structured surfaces.*

The use of etching, oxidation, synthesis and self-assembly processes that enable the processing of a pre-structured surface without the need to manually index the individual elements – *This procedure would be able to process a complete part all at once has a significant impact on the economic viability of the part manufacture, furthermore, being able to "grow" additional structures on top of existing ones.*

5. Conclusions and potential for future developments

Being able to control surface generation across multiple orders of magnitude, either with single machining processes or by the subsequent or parallel processing with multiple technologies, is a desirable goal for many applications. With the advancement of machining technology, multiscale structured surfaces are slowly starting to emerge in research and development, as they offer the possibility to integrate additional functionality into technical products that is otherwise not possible to achieve. Nevertheless, it is virtually impossible to add a specific functionality using a sub-structure without impairing the functionality of the base structure it is applied on, thus this always implies a trade-off of functionality between the two or more levels of overlapping structures. Despite these possible restrictions, the manufacture of such surfaces is of specific concern, as this is the basis to produce components and parts. In this context, the current state-of-the-art of manufacturing technology has been reviewed in this keynote paper.

In order to assess the manufacturability of these structures, so-called multiscality values were introduced that characterize a hierarchically structured surface in its vertical and lateral extent. If these values exceed certain thresholds, the manufactured surface feature multiscale structures. The higher these values get, the more multiscale the surface is and, in most cases, the more difficult it is to produce it. Obviously, a single machining procedure quickly faces its limits and can only be applied in a specific lateral and vertical size range, as shown in Fig. 46. To increase this size range, technologies and working principles must be combined in multi-step and multi-physics approaches with the specific challenge of requiring multidisciplinary approaches and interdisciplinary research groups to be fully mastered.

Therefore, the manufacture of multiscale structured surfaces is only at a starting point now. Many of the developments presented in this paper have principally shown what is possible with current technologies, but actual products specifically relying on multiscale structured surfaces are only slowly starting to emerge. Although not very common at the moment, a great potential is seen in the combination of synthesis and self-assembly processes that generate nanoscale (and

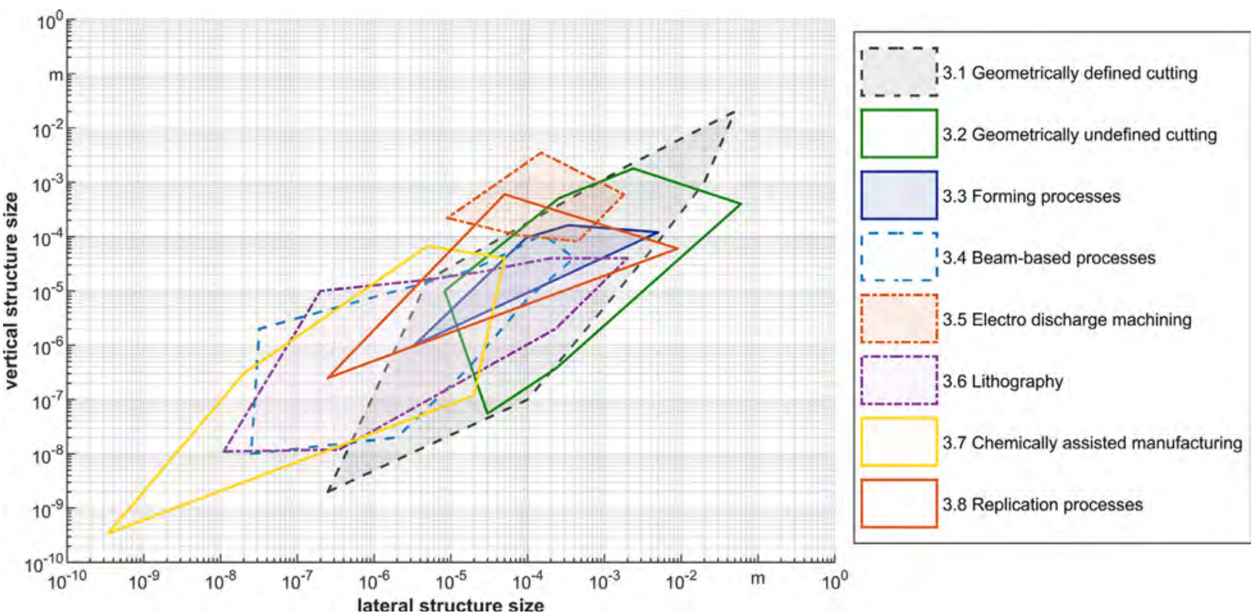

Fig. 46. Size scale of selected manufacturing processes, evaluated from the state of the art.

also multiscale) structures bottom-up with top-down manufacturing processes, such as cutting and forming. Finally, the advancement of additive machining technologies will enable the generation of multiscale structured surfaces for parts that are not only usable in technical applications, but also can directly applied in medical treatments, such as the aforementioned example of producing prostheses that feature the same texture as the intact skin of the patient.

Truly high multiscality grades (>100) are only achievable by combining dedicated manufacturing processes for each structure or functionality. Thus, it is expected for hybrid processes and integrated machining concepts (e.g. combining additive manufacturing and subtractive machining in one machine tool) to steadily gain recognition, with the ultimate goal of manufacturing surfaces with several layers of structural hierarchy that are capable of fully mimicking the functional examples found in nature.

Acknowledgements

The authors gratefully acknowledge contributions received from numerous active researchers. This includes D. Biermann, V. Badami, J. Cao, B. Denkena, C. Evans, P. Groche, F. Hashimoto, G. Hirt, FZ. Fang, L. Orazi and G. Tosello.

The authors wish to thank O. Riemer for his significant contribution to and thorough review of the complete manuscript as well as A.-K. Boinski, T. Dörgeloh, Z. Zhang and T. Zielinski for their essential support within individual sections of this paper.

Parts of the presented work have received funding from the European Union's Horizon 2020 research and innovation program under grant agreement No 767589 (project acronym: ProSurf). The authors express their sincere thanks to the EU.

References

[1] Abeln T (2003) Laserstrukturierung – Verbesserung Der Tribologischen Eigenschaften Von Oberflächen. (in German). *Optische Technologien in der Fahrzeugtechnik: Optische Technologien für die Mikrofertigung* 1810:227–238. VDI Berichte.
[2] Ahmadi SM, Hedayati R, Ashok Kumar Jain RK, Li Y, Leeflang S, Zadpoor AA (2017) Effects of Laser Processing Parameters on the Mechanical Properties, Topology, and Microstructure of Additively Manufactured Porous Metallic Biomaterials: A Vector-Based Approach. *Materials & Design* 134:234–243.
[3] Anguita JV, Ahmad M, Haq S, Allam J, Silva SRP (2016) Ultra-Broadband Light Trapping Using Nanotextured Decoupled Graphene Multilayers. *Science Advances* 2(2):e1501238.
[4] Asakura K, Yan J (2015) Water Repellency Control of Oxygen-Free Copper Surface by Diamond-Cut Micro Grooves. *International Journal of Automation Technology* 9(4):396–402.
[5] Bae W-G, Jeong HE, Kim J (2015) Multiscale Engineered Hierarchical Structures with Precisely Controlled Sizes for Bio-Inspired Cell Culture. *Materials Letters* 159:213–217.
[6] Biermann D, Freiburg D, Hense R, Tillmann W, Stangier D (2015) Influence of Surface Modifications on Friction, Using High-Feed Milling and Wear Resistant PVD-Coating for Sheet-Metal Forming Tools. *KEM* 639:275–282.
[7] Biermann D, Surmann T, Odendahl S, Steiner M, Hense R, Rausch S (2011) Creating Functional Surface Structures by Milling using Self-Excited Tool Vibrations. In: *ASPE Spring Topical Meeting: Structured and Freeform Surfaces*, ASPE, Raleigh, NC, 55–58.
[8] Brandes C, Megne Tague AC, Kroll S, Treccani L, Rezwan K (2016) Gel Casting of Large Area Micro- And Sub-Micropatterned Thin Ceramic Tapes. *Ceramics International* 42(4):5036–5044.
[9] Brinksmeier E, Gläbe R, Schönemann L (2012) Review on Diamond-Machining Processes for the Generation of Functional Surface Structures. *CIRP Journal of Manufacturing Science and Technology* 5(1):1–7.
[10] Brinksmeier E, Riemer O, Schönemann L, Zheng H, Böhmermann F (2014) Microstructuring of Surfaces for Bio-Medical Applications. *Advanced Materials Research* 907:213–224.
[11] Brinksmeier E, Schönemann L (2014) Generation of Discontinuous Microstructures by Diamond Micro Chiseling. *CIRP Annals - Manufacturing Technology* 63 (1):49–52.
[12] Brosius A, Mousavi A (2016) Lubricant Free Deep Drawing Process by Macro Structured Tools. *CIRP Annals - Manufacturing Technology* 65(1):253–256.
[13] Brown CA, Hansen HN, Jiang XJ, Blateyron F, Berglund J, Senin N, Bartkowiak T, Dixon B, Le Goïc G, Quinsat Y, Stemp WJ, Thompson MK, Ungar PS, Zahouani EH (2018) Multiscale Analyses and Characterizations of Surface Topographies. *CIRP Annals - Manufacturing Technology* 67(2):839–862.
[14] Bruzzone AAG, Costa HL, Lonardo PM, Lucca DA (2008) Advances in engineered surfaces for functional performance. *CIRP Annals - Manufacturing Technology* 57 (2):750–769.
[15] Büttner H, Roth R, Wegener K (2018) Limits of Die-Sinking EDM for micro Structuring in W300 Steel with pure Copper Electrodes. *Procedia CIRP* 77:646–649.
[16] Cai Y, Chang W, Luo X, Sousa AML, Lau KHA, Qin Y (2018) Superhydrophobic Structures on 316L Stainless Steel Surfaces Machined by Nanosecond Pulsed Laser. *Precis. Engin.* 52:266–275.
[17] Cao J, Brinksmeier E, Fu M, Gao RX, Liang B, Merklein M, Schmidt M, Yanagimoto J (2019) Manufacturing of Advanced Smart Tooling for Metal Forming. *CIRP Annals - Manufacturing Technology* .
[18] Cao S, Chen H (2017) Nanorods Assembled Hierarchical Urchin-like WO 3 Nanostructures: Hydrothermal Synthesis, Characterization, And Their Gas Sensing Properties. *Journal of Alloys and Compounds* 702:644–648.
[19] Chang T-Y, Yang H, Wu C-H, Chao C-K (2009) Complex Optical Microstructure Fabricated Using Inclined Immersion Lithography. In: *EOS Conferences at the World of Photonics Congress*, 187–190.
[20] Chen W, Zhang X, Liu X, Fang F-Z (2015) Optical Design and Simulation of a Compact Multi-Aperture Camera Based on a Freeform Microlens Array. *Optics Communications* 338:300–306.
[21] Chen X, Wang Y, Wang Z, Liu H, Chi G (2018) Study on Micro Reciprocated Wire-EDM for Complex Indexing Structure. *Procedia CIRP* 68:120–125.
[22] Cheung CF, Liu M, Leach R, Feng X, Zhao C (2018) Hierarchical-information-based characterization of multiscale structured surfaces. *CIRP Annals - Manufacturing Technology* 67(1):539–542.
[23] Choi M, Murillo G, Hwang S, Kim JW, Jung JH, Chen C-Y, Lee M (2017) Mechanical and electrical characterization of PVDF-ZnO hybrid structure for application to nanogenerator. *Nano Energy* 33:462–468.
[24] Chou Y-Y, Lee K-T, Lee Y-C (2016) Fabrication of Hierarchical Anti-Reflective Structures using Polystyrene Sphere Lithography on an as-Cut P-Si Substrate. *Applied Surface Science* 377:81–85.
[25] Dahlmann D, Denkena B (2017) Hybrid tool for high performance structuring and honing of cylinder liners. *CIRP Annals - Manufacturing Technology* 66 (1):113–116.
[26] Davoudinejad A, Cai Y, Pedersen DB, Luo X, Tosello G (2019) Fabrication of micro-structured surfaces by additive manufacturing, with simulation of dynamic contact angle. *Materials & Design* 176:107839.
[27] Denkena B, Grove T, Göttsching T (2015) Grinding with Patterned Grinding Wheels. *CIRP Journal of Manufacturing Science and Technology* 8:12–21.
[28] Denkena B, Grove T, Göttsching T, da Silva EJ, Coelho RT, Filleti R (2015) Enhanced Grinding Performance by means of Patterned Grinding Wheels. *International Journal of Advanced Manufacturing Technology* 77(9–12):1935–1941.
[29] Denkena B, Grove T, Krawczyk T (2016) Tools and Strategies for Grinding of Riblets on Freeformed Compressor Blades. *Procedia CIRP* 55:182–187.
[30] Denkena B, Grove T, Maiss O, Suntharakumaran V (2017) New tool Concept For Grinding a Plateau-Like Surface for Tribological Applications. *Production Engineering Research and Development* 11(4–5):419–424.
[31] Denkena B, Grove T, Seibel A (2016) Direct Part Marking by Vibration Assisted Face Milling. *Procedia Technology* 26:185–191.
[32] Denkena B, Kästner J, Wang B (2010) Advanced microstructures and its production through cutting and grinding. *CIRP Annals - Manufacturing Technology* 59 (1):67–72.
[33] Denkena B, Köhler J, Göttsching T (2013) Influence of Micro Patterned Grinding Wheels on the Work Piece Quality. In: *13th Euspen International Conference*, 249–252.
[34] Denkena B, Köhler J, Kästner J, Göttsching T, Dinkelacker F, Ulmer H (2013) Efficient Machining of Microdimples for Friction Reduction. *Journal of Micro and Nano-Manufacturing* 1(1):11003.
[35] Denkena B, Köhler J, Krawczyk T (2014) Grinding of Riblet Structures on Free Formed Compressor Blades. *Advanced Materials Research* 907:463–473.
[36] Denkena B, Köhler J, Mörke T, Gümmer O (2012) High-Performance Cutting of Micro Patterns. *Procedia CIRP* 1:144–149.
[37] Denkena B, Köhler J, Wang B (2010) Manufacturing of functional riblet structures by profile grinding. *CIRP Journal of Manufacturing Science and Technology* 3 (1):14–26.
[38] Denkena B, de Leon L, Kästner J (2010) Precise Machining of Micro Dimples in Large Scale Areas. in Spaan H, Shore P, van Brussel H, Burke T, (Eds.) *10th euspen International Conference*, 111–115.
[39] Denkena B, de Leon L, Wang B (2009) Grinding of microstructured functional surfaces: a novel strategy for dressing of microprofiles. *Production Engineering Research and Development* 3(1):41–48.
[40] Durret J, Szkutnik P-D, Frolet N, Labau S, Gourgon C (2018) Superhydrophobic polymeric films with hierarchical structures produced by nanoimprint (NIL) and plasma roughening. *Applied Surface Science* 445:97–106.
[41] Elsner-Dörge F, Riemer O, Brinksmeier E (2014) Robot-Assisted Vibration Polishing of NiCo Retroreflector Moulds. *Advanced Materials Research* 1018:175–181.
[42] Evans CJ, Bryan JB (1999) "Structured", "Textured" or "Engineered" Surfaces. *CIRP Annals - Manufacturing Technology* 48(2):541–556.
[43] Fang F-Z, Liu YC (2004) On minimum exit-burr in micro cutting. *Journal of Micromechanics and Microengineering* 14(7):984–988.
[44] Fang F-Z, Wu H, Liu XD, Liu YC, Ng ST (2003) Tool geometry study in micromachining. *Journal of Micromechanics and Microengineering* 13(5):726–731.
[45] Fang F-Z, Xiong Z, Hu XT (2006) An experimental study of micromachining step-mirrors for laser-diode beam shaping. *Journal of Micromechanics and Microengineering* 16(2):214–218.
[46] Fang F-Z, Xu ZW, Hu XT, Wang CT, Luo XG, Fu YQ (2010) Nano-photomask fabrication using focused ion beam direct writing. *CIRP Annals - Manufacturing Technology* 59(1):543–546.
[47] Fang F-Z, Zhang N, Zhang X (2016) Precision injection molding of freeform optics. *Advanced Optical Technologies* 5(4):19743.
[48] Fang F-Z, Zhang XD, Gao W, Guo YB, Byrne G, Hansen HN (2017) Nanomanufacturing—Perspective and applications. *CIRP Annals - Manufacturing Technology* 66 (2):683–705.
[49] Fang F-Z, Zhang XD, Weckenmann A, Zhang GX, Evans CJ (2013) Manufacturing and measurement of freeform optics. *CIRP Annals - Manufacturing Technology* 62 (2):823–846.

[50] Flucke C, Osmer J, Lünemann B, Schönemann L, Brinksmeier E (2009) Scaling in Machining of Optics with Reflective to Diffractive Function. in Brussel Hvan, Brinksmeier E, Spaan H, (Eds.) *9th euspen international conference*, 17–20.
[51] Fu Y, Liu Y, Zhou X, Xu Z, Fang F-Z (2010) Experimental Investigation of Superfocusing of Plasmonic Lens with Chirped Circular Nanoslits. *Optics express* 18 (4):3438–3443.
[52] Gao T, Xu Z, Fang F-Z, Gao W, Zhang Q, Xu X (2012) High performance surface-enhanced Raman scattering substrates of Si-based Au film developed by focused ion beam nanofabrication. *Nanoscale Research Letters* 7(1):399.
[53] Gao W, Araki T, Kiyono S, Okazaki Y, Yamanaka M (2003) Precision Nano-Fabrication and Evaluation of a Large Area Sinusoidal Grid Surface for a Surface Encoder. *Precision Engineering* 27(3):289–298.
[54] Gao W, Haitjema H, Fang FZ, Leach RK, Cheung CF, Savio E, Linares JM (2019) On-Machine and In-Process Surface Metrology for Precision Manufacturing. *CIRP Annals - Manufacturing Technology* 68(2):843–866.
[55] Gnilitskyi I, Derrien TJ-Y, Levy Y, Bulgakova NM, Mocek T, Orazi L (2017) High-Speed Manufacturing of Highly Regular Femtosecond Laser-Induced Periodic Surface Structures: Physical Origin of Regularity. *Scientific Reports* 7(1):8485.
[56] Gnilitskyi I, Gruzdev V, Bulgakova NM, Mocek T, Orazi L (2016) Mechanisms of high-regularity periodic structuring of silicon surface by sub-MHz repetition rate ultrashort laser pulses. *Applied Physics Letters* 109(14):143101.
[57] Gnilitskyi I, Rotundo F, Martini C, Pavlov I, Ilday S, Vovk E, FÖ Ilday, Orazi L (2016) Nano Patterning of AISI 316L Stainless Steel with Nonlinear Laser Lithography: sliding Under Dry and Oil-Lubricated Conditions. *Tribology International* 99:67–76.
[58] Greco A, Raphaelson S, Ehmann K, Wang QJ, Lin C (2009) Surface Texturing of Tribological Interfaces Using the Vibromechanical Texturing Method. *Journal of Manufacturing Science and Engineering* 131(6):61005.
[59] Guo P, Lu Y, Ehmann KF, Cao J (2014) Generation of Hierarchical Micro-Structures For Anisotropic Wetting By Elliptical Vibration Cutting. *CIRP Annals - Manufacturing Technology* 63(1):553–556.
[60] Guo R, Yu Y, Xie Z, Liu X, Zhou X, Gao Y, Liu Z, Zhou F, Yang Y, Zheng Z (2013) Matrix-Assisted Catalytic Printing for the Fabrication of Multiscale, Flexible, Foldable, And Stretchable Metal Conductors. *Advanced materials (Deerfield Beach, Fla.)* 25(24):3343–3350.
[61] Han Q, Fu Y, Jin L, Zhao J, Xu Z, Fang F-Z, Gao J, Yu W (2015) Germanium Nano-pyramid Arrays Showing Near-100% Absorption in the Visible Regime. *Nano Research* 8(7):2216–2222.
[62] Hansen HN, Hocken RJ, Tosello G (2011) Replication of Micro and Nano Surface Geometries. *CIRP Annals - Manufacturing Technology* 60(2):695–714.
[63] Hashimoto F, Zhou RS (2017) Design of Dimpled Engineering Surfaces for Improving Lubrication Performance in Rolling-Sliding Contacts. *IJAT* 8(1):44.
[64] He Y, Xiao X, Wu Y, Fu J-z (2015) A Facile and Low-Cost Micro Fabrication Material: Flash Foam. *Sci Rep* 5:13522.
[65] He ZR, Luo ST, Liu CS, Jie XH, Lian WQ (2019) Hierarchical Micro/Nano Structure Surface Fabricated by Electrical Discharge Machining for Anti-Fouling Application. *Journal of Materials Research and Technology* 8(5):3878–3890.
[66] Hense R (2013) Using Chatter Vibrations in Milling to Create Tribo-Functional Surfaces for Sheet-Bulk Metal Forming Tools. *Advanced Materials Research* 769:263–270.
[67] Hense R, Wels C, Kersting P, Vierzigmann U, Löffler M, Biermann D, Merklein M (2015) High-Feed Milling of Tailored Surfaces for Sheet-Bulk Metal Forming Tools. *Production Engineering Research and Development* 9(2):215–223.
[68] Herrmann M, Böhmermann F, Hasselbruch H, Kuhfuss B, Riemer O, Mehner A, Zoch H-W (2017) Forming without Lubricant – Functionalized Tool Surfaces for Dry Forming Applications. *Procedia Manufacturing* 8:533–540.
[69] Hnilova M, Karaca BT, Park J, Jia C, Wilson BR, Sarikaya M, Tamerler C (2012) Fabrication Of Hierarchical Hybrid Structures Using Bio-Enabled Layer-By-Layer Self-Assembly. *Biotechnology and Bioengineering* 109(5):1120–1130.
[70] Hu X, Xu Z, Li K, Fang F-Z, Wang L (2015) Fabrication of a Au–Polystyrene Sphere Substrate With Three-Dimensional Nanofeatures For Surface-Enhanced Raman spectroscopy. *Applied Surface Science* 355:1168–1174.
[71] Huang H, Yan J (2018) Multi-Scale Dimple Creation On Metallic Glass by a Two-Step Method Involving Nanoindentation and Polishing. *Applied Surface Science* 462:565–574.
[72] Huang M-J, Yang C-R, Lee H-S, Liu H-L (2014) Fabrication of Novel Hybrid Antireflection Structures for Solar Cells. *Solar Energy* 107:489–494.
[73] Huang R, Zhang X, Kumar AS, Liu K, Rahman M (2017) Profile Evaluation of Radial Fresnel Lens Directly Machined on Roller Molds by Rotating-Tool Diamond Turning. *Precision Engineering* 50:44–52.
[74] Huang R, Zhang X, Neo WK, Kumar AS, Liu K (2018) Ultra-Precision Machining of Grayscale Pixelated Micro Images on Metal Surface. *Precision Engineering* 52:211–220.
[75] Huang R, Zhang X, Rahman M, Kumar AS, Liu K (2015) Ultra-Precision Machining of Radial Fresnel Lens on Roller Moulds. *CIRP Annals - Manufacturing Technology* 64(1):121–124.
[76] Huerta-Murillo D, Aguilar-Morales AI, Alamri S, Cardoso JT, Jagdheesh R, Lasagni AF, Ocaña JL (2017) Fabrication of Multi-Scale Periodic Surface Structures on Ti-6Al-4V by Direct Laser Writing and Direct Laser Interference Patterning for Modified Wettability Applications. *Optics and Lasers in Engineering* 98:134–142.
[77] Huovinen E, Takkunen L, Suvanto M, Pakkanen TA (2014) Fabrication and quantitative roughness analysis of hierarchical multiscale polymer surface structures. *Journal of Micromechanics and Microengineering* 24(5):55017.
[78] Jheng Y-S, Lee Y-C (2016) Fabrication of Micro/Nano Hierarchical Structures with Analysis on the Surface Mechanics. *Applied Surface Science* 384:393–399.
[79] Jones CW, Leach RK (2008) Adding a Dynamic Aspect to Amplitude–Wavelength Space. *Measurement Science & Technology* 19(5):55105.
[80] Kang J-M, Wei M-K, Lin H-Y, Lee J-H, Lin H-Y, Tsai J-H, Wu T-C (2010) Shape-Controlled Microlens Arrays Fabricated By Diffuser Lithography. *Microelectronic Engineering* (5–8):1420–1423.
[81] Karpuschewski B, Pieper H-J, Welzel F, Risse K (2012) Alternative Strategies In Finishing Cylinder Running Surfaces. *CIRP Annals - Manufacturing Technology* 61 (1):559–562.
[82] Karpuschewski B, Welzel F, Risse K, Schorgel M, Kreter S (2016) Potentials for Improving Efficiency of Combustion Engines Due to Cylinder Liner Surface Engineering. *Procedia CIRP* 46:258–265.
[83] Kersting P, Gröbel D, Merklein M, Sieczkarek P, Wernicke S, Tekkaya AE, Krebs E, Freiburg D, Biermann D, Weikert T, Tremmel S, Stangier D, Tillmann W, Matthias S, Reithmeier E, Löffler M, Beyer F, Willner K (2016) Experimental and numerical analysis of tribological effective surfaces for forming tools in Sheet-Bulk Metal Forming. *Production Engineering Research and Development* 10(1):37–50.
[84] Kim JH, Chang SS, Lim G (2014) Fabrication of Multi-Scale Structures with Multiple X-Ray Masks and Synchrotron Hard X-Ray Irradiations. *Current Applied Physics* 14(5):833–837.
[85] Kim J-H, Mirzaei A, Kim HW, Kim SS (2018) Realization of Superhydrophobic Aluminum Surfaces with Novel Micro-Terrace Nano-Leaf Hierarchical Structure. *Applied Surface Science* 451:207–217.
[86] Klocke F, Feldhaus B, Mader S (2007) Development of an Incremental Rolling Process for the Production of Defined Riblet Surface Structures. *Production Engineering Research and Development* 1(3):233–237.
[87] Ko D-H, Tumbleston JR, Henderson KJ, Euliss LE, DeSimone JM, Lopez R, Samulski ET (2011) Biomimetic Microlens Array with Antireflective "moth-eye" Surface. *Soft Matter* 7(14):6404.
[88] Kobayashi T, Sera H, Wakabayashi T, Endo H, Takushima Y, Yan J (2018) Surface Flattening and Nanostructuring of Steel by Picosecond Pulsed Laser Irradiation. *Nanomanufacturing and Metrology* 62:203.
[89] Köhler J, Seibel A (2015) FTS-based Face Milling of Micro Structures. *Procedia CIRP* 28:58–63.
[90] Kong LB, Cheung CF (2011) Design, Fabrication and Measurement of Ultra-Precision Micro-Structured Freeform Surfaces. *Computers & Industrial Engineering* 61 (1):216–225.
[91] Kong LB, Cheung CF, Lee WB (2016) A theoretical and Experimental Investigation Of Orthogonal Slow Tool Servo Machining Of Wavy Microstructured Patterns On Precision Rollers. *Precision Engineering* 43:315–327.
[92] Kong LB, Cheung CF, To S (2012) Design, Fabrication And Characterization Of Three-Dimensional Patterned Microstructured Surfaces With Self-Cleaning Properties From Hydrophilic Materials. *Proceedings of the Institution of Mechanical Engineers, Part B: Journal of Engineering Manufacture* 226(9):1536–1549.
[93] Kong LB, Cheung CF, To S, Cheng CT (2013) Modeling and Characterization Of Generation Of 3d Micro-Structured Surfaces With Self-Cleaning And Optical Functions. *Optik - International Journal for Light and Electron Optics* 124 (17):2848–2853.
[94] Krasnikova IV, Mishakov IV, Vedyagin AA, Krivoshapkin PV, Korneev DV (2018) Hierarchically Structured Carbon-Carbon Nanocomposites: The Preparation Aspects. *Composites Communications* 7:65–68.
[95] Kühne S, Haskic K, Lemke S, Schmidt M (2014) Fabrication and Characterization Of Machined 3D Diffractive Optical Elements. *Microsystem Technologies* 20 (10–11):2103–2107.
[96] Kwak MK, Pang C, Jeong H-E, Kim H-N, Yoon H, Jung H-S, Suh K-Y (2011) Towards the Next Level of Bioinspired Dry Adhesives: new Designs and Applications. *Advanced Functional Materials* 21(19):3606–3616.
[97] Lee J, Park H-H, Choi K-B, Kim G, Lim H (2014) Fabrication of Hybrid Structures Using UV Roll-Typed Liquid Transfer Imprint Lithography for Large Areas. *Microelectronic Engineering* 127:72–76.
[98] Lee P, Ham J, Lee J, Hong S, Han S, Suh YD, Lee SE, Yeo J, Lee SS, Lee D, Ko SH (2014) Highly Stretchable or Transparent Conductor Fabrication by a Hierarchical Multiscale Hybrid Nanocomposite. *Advanced Functional Materials* 24 (36):5671–5678.
[99] Li G, Xu Z, Fang F-Z, Wu W, Xing X, Li W, Liu H (2013) Micro cutting of V-shaped cylindrical grating template for roller nano-imprint. *Journal of Materials Processing Technology* 213(6):895–904.
[100] Li L, Yi AY (2009) Microfabrication on a curved surface using 3D microlens array projection. *Journal of Micromechanics and Microengineering* 19(10):105010.
[101] Lietmeyer C, Denkena B, Krawczyk T, Kling R, Overmeyer L, Wojakowski B, Reithmeier E, Scheuer R, Vynnyk T, Seume JR (2013) Recent Advances in Manufacturing of Riblets on Compressor Blades and Their Aerodynamic Impact. *Journal of Turbomachinery* 135(4):41008.
[102] Lim HS, Wong YS, Rahman M, Edwin Lee MK (2003) A study on the machining of high-aspect ratio micro-structures using micro-EDM. *Journal of Materials Processing Technology* 140(1–3):318–325.
[103] Liu B, Wang W, Jiang G, Mei X, Wang Z, Wang K, Cui J (2016) Study on Hierarchical Structured PDMS for Surface Super-Hydrophobicity Using Imprinting With Ultrafast Laser Structured Models. *Applied Surface Science* 364:528–538.
[104] Liu C-W, Yan J, Lin S-C (2016) Diamond Turning Of High-Precision Roll-To-Roll Imprinting Molds for Fabricating Subwavelength Gratings. *Optical Engineering* 55(6):64105.
[105] Liu K, Jiang L (2011) Bio-inspired design of multiscale structures for function integration. *Nano Today* 6(2):155–175.
[106] Liu X, Zhou T, Zhang L, Zhou W, Yu J, Lee LJ, Yi AY (2019) 3D fabrication of spherical microlens arrays on concave and convex silica surfaces. *Microsystem Technologies* 25(1):361–370.
[107] Liu Y, Fu Y, Zhou X, Xu Z, Fang F-Z, Hu X (2011) Experimental Study of Indirect Phase Tuning-Based Plasmonic Structures for Finely Focusing. *Plasmonics* 6 (2):227–233.
[108] Löffler M, Andreas K, Engel U, Schulte R, Groebel D, Krebs E, Freiburg D, Biermann D, Stangier D, Tillmann W, Weikert T, Wartzack S, Tremmel S, Lucas H, Denkena B, Merklein M (2016) Tribological measures for controlling material flow in sheet-bulk metal forming. *Production Engineering Research and Development* 10(4–5):459–470.
[109] Lucas H, Denkena B, Grove T, Krebs E, Kersting P, Freiburg D, Biermann D (2015) Analysis of Residual Stress States of Structured Surfaces Manufactured by High-Feed and Micromilling. *HTM* 70(4):183–189.
[110] Lucca DA, Klopfstein MJ, Mejia OR, Rossettini L, De Luca L (2004) Investigation of the Near Surface Mechanical Properties of Ammonium Perchlorate Using

Nanoindentation. in De Luca L, Galfetti L, Pesce-Rodriguez R, (Eds.) *Novel Energetic Materials and Applications*, Grafiche G.S.S. Arzago d'Adda, BG, Italy.
[111] Malshe A, Rajurkar KP, Samant A, Hansen HN, Bapat S, Jiang W (2013) Bio-inspired functional surfaces for advanced applications. *CIRP Annals - Manufacturing Technology* 62(2):607–628.
[112] Malshe AP, Bapat S, Rajurkar KP, Haitjema H (2018) Bio-inspired textures for functional applications. *CIRP Annals - Manufacturing Technology* 67(2):627–650.
[113] Manaf ARA, Sugiyama T, Yan J (2017) Design and Fabrication of Si-HDPE Hybrid Fresnel Lenses for Infrared Imaging Systems. *Optics Express* 25(2):1202–1220.
[114] Masui S, Michihata M, Takamasu K, Takahashi S (2019) Fabrication of Nano- and Micro- Structured Surface Using Spatial Beat of Evanescent Wave Interference Lithography. In: *Euspen's 19th International Conference & Exhibition*, euspen, .
[115] Matsumura T, Iida F, Hirose T, Yoshino M (2012) Micro machining for control of wettability with surface topography. *Journal of Materials Processing Technology* 212(12):2669–2677.
[116] Matsumura T, Serizawa M, Ogawa T, Sasaki M (2015) Surface dimple machining in whirling. *Journal of Manufacturing Systems* 37:487–493.
[117] Matsumura T, Takahashi S (2012) Micro Dimple Milling on Cylinder Surfaces. *Journal of Manufacturing Processes* 14(2):135–140.
[118] Meier A (2015) Diamond Turning of Diffractive Microstructures. *Precision Engineering* 42:253–260.
[119] Meier A, Riemer O, Brinksmeier E (2016) Diamond Machining of Holograms Using Fine Rectangular Shaped Cutting Tools. *International Journal of Automation Technology* 10(1):16–22.
[120] Moriwaki T, Shamoto E (1995) Ultrasonic Elliptical Vibration Cutting. *CIRP Annals - Manufacturing Technology* 44(1):31–34.
[121] Mukaida M, Yan J (2017) Fabrication of Hexagonal Microlens Arrays on Single-Crystal Silicon Using the Tool-Servo Driven Segment Turning Method. *Micromachines* 8(11):323.
[122] Murr LE, Gaytan SM, Ramirez DA, Martinez E, Hernandez J, Amato KN, Shindo PW, Medina FR, Wicker RB (2012) Metal Fabrication by Additive Manufacturing Using Laser and Electron Beam Melting Technologies. *Journal of Materials Science & Technology* 28(1):1–14.
[123] Orazi L, Gnilitskyi I, Pavlov I, Serro AP, Ilday S, Ilday FO (2015) Nonlinear laser lithography to control surface properties of stainless steel. *CIRP Annals - Manufacturing Technology* 64(1):193–196.
[124] Orazi L, Gnilitskyi I, Serro AP (2017) Laser Nanopatterning for Wettability Applications. *Journal of Micro and Nano-Manufacturing* 5(2):21008.
[125] Pang K, Fang F-Z, Le Song Zhang Y, Zhang H (2017) Bionic Compound Eye for 3D Motion Detection Using an Optical Freeform Surface. *Journal of the Optical Society of America B: Optical Physics* 34(5):B28.
[126] Pang K, Le Song Fang F-Z, Zhang Y, Zhang H (2016) An Imaging System with a Large Depth of Field Based on an Overlapped Micro-Lens Array. *CIRP Annals - Manufacturing Technology* 65(1):471–474.
[127] Park J, Fujita H, Kim B (2011) Fabrication of Metallic Microstructure on Curved Substrate by Optical Soft Lithography and Copper Electroplating. *Sensors and Actuators A: Physical* 168(1):105–111.
[128] Pei J, Liu Y, Zhu Y, Zhang L, Zhuang X, Wu S (2018) Machining Strategy and Key Problems for 3D Structure of Micro-EDM by Fix-length Compensation Method with Tubular Electrodes. *Procedia CIRP* 68:802–807.
[129] Peng L, Zhang C, Wu H, Yi P, Lai X, Ni J (2016) Continuous Fabrication of Multiscale Compound Eyes Arrays With Antireflection and Hydrophobic Properties. *IEEE Trans. Nanotechnology* 15(6):971–976.
[130] Raut HK, Dinachali SS, Loke YC, Ganesan R, Ansah-Antwi KK, Góra A, Khoo EH, Ganesh VA, Saifullah MSM, Ramakrishna S (2015) Multiscale Ommatidial Arrays with Broadband and Omnidirectional Antireflection and Antifogging Properties By Sacrificial Layer Mediated Nanoimprinting. *ACS Nano* 9(2):1305–1314.
[131] Ren B, Wan Y, Liu Z, Wang G, Ge P (2018) Preparation of Superhydrophobic Titanium Surfaces Via The Combined Modification of Hierarchical Micro-Nano Patterning And Fluorination. In: *6th International Conference on Nanomanufacturing*, nanoMan2018, .
[132] Rosén S, Thomas TR, Rosén B-G (2014) The Stedman Diagram Revisited. *Surface Topography: Metrology and Properties* 2(1):14005.
[133] Rosenkranz A, Gruetzmacher PG, Szurdak A, Gachot C, Hirt G, Muecklich F (2016) Synergetic Effect of Laser Patterning and Micro Coining for Controlled Lubricant Propagation. *Surface Topography: Metrology and Properties* 4(3):34008.
[134] Rosenkranz A, Szurdak A, Gachot C, Hirt G, Mücklich F (2016) Friction Reduction Under Mixed and Full Film EHL Induced by Hot Micro-Coined Surface Patterns. *Tribology International* 95:290–297.
[135] Rotella G, Orazi L, Alfano M, Candamano S, Gnilitskyi I (2017) Innovative High-Speed Femtosecond Laser Nano-Patterning For Improved Adhesive Bonding of Ti6Al4V titanium alloy. *CIRP Journal of Manufacturing Science and Technology* 18:101–106.
[136] Saxena I, Liu J, Ehmann K, Cao J (2015) Periodic Surface Pattern Fabrication Via Biprism Interference Micro-Machining. *Surface Topography: Metrology and Properties* 3(4):45006.
[137] Schönemann L, Brinksmeier E (2018) Micro Chiseling of Retroreflective Arrays. in Yan J, (Ed.) *Micro and Nano Fabrication Technology*, Springer Singapore, Singapore, 1–29.
[138] Schönemann L, Preuss W (2013) Mold Structuring by Diamond Machining. in Brinksmeier E, Gläbe R, Riemer O, (Eds.) *Fabrication of Complex Optical Components: From mold design to product*, Springer, Berlin Heidelberg, 53–66.
[139] Seol Y-J, Lee H, Copus JS, Kang H-W, Cho D-W, Atala A, Lee SJ, Yoo JJ (2018) 3D Bioprinted Biomask for Facial Skin Reconstruction. *Bioprinting* 10:e00028.
[140] Serizawa M, Suzuki M, Matsumura T (2015) Microthreading in Whirling. *Journal of Micro and Nano-Manufacturing* 3(4):41001.
[141] Shore P (2008) Ultra Precision Surfaces. In: *23rd ASPE Annual Meeting and 12th ICPE*, 75–78.
[142] Sieczkarek P, Kwiatkowski L, Tekkaya AE, Krebs E, Kersting P, Tillmann W, Herper J (2013) Innovative Tools to Improve Incremental Bulk Forming Processes. *KEM* 554-557:1490–1497.
[143] Sieczkarek P, Wernicke S, Gies S, Tekkaya AE, Krebs E, Wiederkehr P, Biermann D, Tillmann W, Stangier D (2016) Wear Behavior of Tribologically Optimized Tool Surfaces for Incremental Forming Processes. *Tribology International* 104:64–72.
[144] Sieczkarek P, Wernicke S, Gies S, Tekkaya AE, Krebs E, Wiederkehr P, Biermann D, Tillmann W, Stangier D (2017) Improvement Strategies for the Formfilling in Incremental Gear Forming Processes. *Production Engineering Research and Development* 11(6):623–631.
[145] Stedman M (1987) Basis for Comparing the Performance of Surface-Measuring Machines. *Precision Engineering* 9(3):149–152.
[146] Stedman M (1987) Mapping The Performance Of Surface-Measuring Instruments. in Weck M, (Ed.). *Proc. SPIE: The Hague International Symposium*, SPIE, 138.
[147] Stewart DK (1991) *Wood-turning chatter tool: United States Patent*, 065.
[148] Sun J, Luo X, Chang W, Ritchie JM, Chien J, Lee A (2012) Fabrication of Periodic Nanostructures by Single-Point Diamond Turning with Focused Ion Beam Built Tool Tips. *Journal of Micromechanics and Microengineering* 22(11):115014.
[149] Sun T, Feng L, Gao X, Jiang L (2005) Bioinspired Surfaces with Special Wettability. *Accounts of Chemical Research* 38(8):644–652.
[150] Sun Y, Shimada K, Xu S, Mizutani M, Kuriyagawa T (2018) Friction Reduction by Micro-Textured Surfaces in Lubrication. *International Journal of Automation Technology* 12(4):603–610.
[151] Suzuki N, Haritani M, Yang J, Hino R, Shamoto E (2007) Elliptical Vibration Cutting of Tungsten Alloy Molds for Optical Glass Parts. *CIRP Annals - Manufacturing Technology* 56(1):127–130.
[152] Szurdak A, Hirt G (2015) Finite Element Analysis of Manufacturing Micro Lubrication Pockets in High Strength Steels by Hot Micro-Coining. *Steel Research Int* 86(3):257–265.
[153] Ta QTH, Park S, Noh J-S (2017) Ag Nanowire/ZnO Nanobush Hybrid Structures For Improved Photocatalytic Activity. *Journal of colloid and interface science* 505:437–444.
[154] Takayama N, Ishizuka J, Yan J (2018) Microgrooving of a Single-Crystal Diamond Tool Using a Picosecond Pulsed Laser and Some Cutting Tests. *Precision Engineering* 53:252–262.
[155] Tillmann W, Hagen L, Stangier D, Laemmerhirt I-A, Biermann D, Kersting P, Krebs E (2015) Wear Behavior of Bio-Inspired and Technologically Structured HVOF Sprayed NiCrBSiFe coatings. *Surface and Coatings Technology* 280: 16–26.
[156] Tillmann W, Stangier D, Lopes-Dias N-F, Biermann D, Krebs E (2017) Adjustment of Friction by Duplex-Treated, Bionic Structures for Sheet-Bulk Metal Forming. *Tribology International* 111:9–17.
[157] To S, Zhu Z, Zeng W (2015) Novel end-fly-cutting-servo system for deterministic generation of hierarchical micro–nanostructures. *CIRP Annals - Manufacturing Technology* 64(1):133–136.
[158] Totsu K, Fujishiro K, Tanaka S, Esashi M (2006) Fabrication of Three-Dimensional Microstructure using Maskless Gray-Scale Lithography. *Sensors and Actuators A: Physical* 130-131:387–392.
[159] Uhlmann E, Kühne S, Jagodzinski M (2016) Influence of the Rake Angle on the Surface Formation During Micro Shaping of Submicron Optical Structures in Aulayers. *Euspen ICE* 2016.
[160] Uhlmann E, Mullany B, Biermann D, Rajurkar KP, Hausotte T, Brinksmeier E (2016) Process chains for high-precision components with micro-scale features. *CIRP Annals - Manufacturing Technology* 65(2):549–572.
[161] Uhlmann E, Perfilov I (2018) Machine Tool and Technology for Manufacturing of Micro-structures by Micro Dry Electrical Discharge Milling. *Procedia CIRP* 68:825–830.
[162] Wang BB, Qu XL, Zheng K, Levchenko I, Keidar M, Zhu MK, Xu S, Ostrikov K (2017) C and O doped BN Nanoflake and Nanowire Hybrid Structures for Tuneable Photoluminescence. *Journal of Alloys and Compounds* 705:691–699.
[163] Wang J, Qian J, Ferraris E, Reynaerts D (2017) In-situ Process Monitoring and Adaptive Control for Precision Micro-EDM Cavity Milling. *Precision Engineering* 47:261–275.
[164] Wang W, Zhao W, Wang K, Wang L, Wang X, Wang S, Zhang C, Bai J (2017) On Hydrophilicity Improvement of the Porous Anodic Alumina Film by Hybrid Nano/Micro Structuring. *Applied Surface Science* 416:710–715.
[165] Welzel F (2014) *Tribologische Optimierung von Zylinderlaufflächen in Verbrennungsmotoren aus fertigungstechnischer Sicht (in German)* PhD thesis. University of Magdeburg.
[166] Xia F, Jiang L (2008) Bio-Inspired, Smart, Multiscale Interfacial Materials. *Advanced Materials* 20(15):2842–2858.
[167] Xie J, Li YH, Yang LF (2015) Study on 5-axial milling on microstructured freeform surface using the macro-ball cutter patterned with micro-cutting-edge array. *CIRP Annals - Manufacturing Technology* 64(1):101–104.
[168] Xie J, Luo MJ, Wu KK, Yang LF, Li DH (2013) Experimental Study on Cutting Temperature and Cutting Force in Dry Turning of Titanium Alloy using a Non-Coated Micro-Grooved Tool. *International Journal of Machine Tools and Manufacture* 73:25–36.
[169] Xie J, Wu K, Cheng J, Li P, Zheng J (2015) The Micro-Optic Photovoltaic Behavior of Solar Cell Along With Microlens Curved Glass Substrate. *Energy Conversion and Management* 96:315–321.
[170] Xie J, Zhuo YW, Tan TW (2011) Experimental Study on Fabrication and Evaluation of Micro Pyramid-Structured Silicon Surface using a V-tip of Diamond Grinding Wheel. *Precision Engineering* 35(1):173–182.
[171] Xing Y, Deng J, Wang X, Ehmann K, Cao J (2016) Experimental Assessment of Laser Textured Cutting Tools in Dry Cutting of Aluminum Alloys. *Journal of Manufacturing Science and Engineering* 138(7):71006.
[172] Xu L, Zeng W, Li Y (2018) Synthesis of Morphology and Size-Controllable SnO 2 Hierarchical Structures and Their Gas-Sensing Performance. *Applied Surface Science* .
[173] Xu S, Kuriyagawa T, Shimada K, Mizutani M (2017) Recent Advances in Ultrasonic-Assisted Machining for the Fabrication of Micro/Nano-Textured Surfaces. *Frontiers in Mechanical Engineering* 12(1):33–45.

[174] Xu Z, Fang F-Z, Gao H, Zhu Y, Wu W, Weckenmann A (2012) Nano Fabrication of Star Structure for Precision Metrology Developed by Focused Ion Beam Direct Writing. *CIRP Annals - Manufacturing Technology* 61(1):511–514.
[175] Xu ZW, Fang F-Z, Fu YQ, Zhang SJ, Han T, Li JM (2009) Fabrication of Micro/Nano-Structures using Focused Ion Beam Implantation and XeF 2 Gas-Assisted Etching. *Journal of Micromechanics and Microengineering* 19(5):54003.
[176] Xu ZW, Fang F-Z, Zhang SJ, Zhang XD, Hu XT, Fu YQ, Li L (2010) Fabrication of Micro DOE using Micro Tools Shaped with Focused Ion Beam. *Optics Express* 18 (8):8025–8032.
[177] Xue B, Yan Y (2018) Microstructures Fabricated by the Revolving Tip-Based Machining Method and Their Applications. In: *6th International Conference on Nanomanufacturing*, nanoMan, , 2018.
[178] Yan G, You K, Fang F-Z (2018) Ultraprecision Grinding of Small-Aperture Concave Aspheric Mould Insert with Tilt Axis Method. *Procedia CIRP* 71:505–510.
[179] Yan J, Imoto Y (2018) Nanoscale Surface Patterning of Diamond Utilizing Carbon Diffusion Reaction with a Microstructured Titanium Mold. *CIRP Annals - Manufacturing Technology* 67(1):181–184.
[180] Yan J, Oowada T, Zhou T, Kuriyagawa T (2009) Precision Machining of Microstructures on Electroless-Plated NiP Surface for Molding Glass Components. *Journal of Materials Processing Technology* 209(10):4802–4808.
[181] Yan J, Watanabe K, Nakagawa Y (2013) Fabrication of Thin-Film Fresnel Optics by Combining Diamond Turning and Photolithographic Processes. *International Journal of Automation Technology* 7(4):385–390.
[182] Yan J, Zhang Z, Kuriyagawa T, Gonda H (2010) Fabricating Micro-Structured Surface by Using Single-Crystalline Diamond Endmill. *International Journal of Advanced Manufacturing Technology* 51(9–12):957–964.
[183] Yang S, Aizenberg J (2005) Microlens Arrays with Integrated Pores. *Materials Today* 8(12):40–46.
[184] Yang W, Wang X, Li H, Song X (2017) Effects of Hierarchical Structures and Insulating Liquid Media on Adhesion. *Applied Surface Science* 423:891–899.
[185] Yin L, Ramesh K, Wan S, Liu XD, Huang H, Liu YC (2004) Abrasive Flow Polishing of Micro Bores. *Materials and Manufacturing Processes* 19(2):187–207.
[186] Yuan LL (2016) *Flexible Fabrication of Multi-scale Integrated 3D Periodic Nano-structures with Phase Mask* PhD Thesis. University of TorontoToronto.
[187] Yuan LL, Herman PR (2016) Laser Scanning Holographic Lithography for Flexible 3D Fabrication of Multi-Scale Integrated Nano-structures and Optical Biosensors. *Scientific Reports* 6:22294.
[188] Yuan Y, Ehmann KF, Cao J (2017) Surface Texturing–Functionality and Manufacturability. *Procedia Manufacturing* .
[189] Yuan Z, Bin J, Wang X, Peng C, Wang M, Xing S, Xiao J, Zeng J, Xiao X, Fu X, Chen H (2014) Fabrication of superhydrophobic surface with hierarchical multi-scale structure on copper foil. *Surface and Coatings Technology* 254:151–156.
[190] Yue X, Liu W, Wang Y (2018) Freezing Delay, Frost Accumulation and Droplets Condensation Properties of Micro- or Hierarchically-Structured Silicon Surfaces. *International Journal of Heat and Mass Transfer* 126:442–451.
[191] Zeng Z, Wang Y, Wang Z, Shan D, He X (2012) A study of micro-EDM and Micro-ECM Combined Milling for 3D Metallic Micro-Structures. *Precision Engineering* 36(3):500–509.
[192] Zhang AP, Qu X, Soman P, Hribar KC, Lee JW, Chen S, He S (2012) Rapid Fabrication of Complex 3D Extracellular Microenvironments by Dynamic Optical Projection Stereolithography. *Advanced Materials (Deerfield Beach, Fla.)* 24 (31):4266–4270.
[193] Zhang H, Fang F-Z, Gilchrist MD, Zhang N (2018) Filling of High Aspect Ratio Micro Features of a Microfluidic Flow Cytometer Chip Using Micro Injection Moulding. *Journal of Micromechanics and Microengineering* 28(7):75005.
[194] Zhang H, Yang J, Chen B, Liu C, Zhang M, Li C (2015) Fabrication of Superhydrophobic Textured Steel Surface for Anti-Corrosion and Tribological Properties. *Applied Surface Science* 359:905–910.
[195] Zhang J, Suzuki N, Shamoto E (2013) Investigation on Machining Performance of Amplitude Control Sculpturing Method in Elliptical Vibration Cutting. *Procedia CIRP* 8:328–333.
[196] Zhang J, Suzuki N, Wang Y, Shamoto E (2015) Ultra-Precision Nano-Structure Fabrication by Amplitude Control Sculpturing Method In Elliptical Vibration Cutting. *Precision Engineering* 39:86–99.
[197] Zhang L, Xie J, Guo RB, Wu KK, Li P, Zheng JH (2016) Precision and Mirror Micro-Grinding of Micro-Lens Array on Macro-Freeform Glass Substrate for Micro-Photovoltaic Performances. *International Journal of Advanced Manufacturing Technology* 86(1–4):87–96.
[198] Zhang N, Srivastava A, Kirwan B, Byrne R, Fang F-Z, Browne DJ, Gilchrist MD (2015) Manufacturing Microstructured Tool Inserts for the Production Of Polymeric Microfluidic Devices. *Journal of Micromechanics and Microengineering* 25 (9):95005.
[199] Zhang N, Zhang H, Stallard C, Fang F-Z, Gilchrist MD (2018) Replication integrity of micro features using variotherm and vacuum assisted microinjection moulding. *CIRP Journal of Manufacturing Science and Technology* 23:20–38.
[200] Zhang N, Zhang H, Zhang H, Fang F-Z, Gilchrist MD (2018) Geometric Replication Integrity of Micro Features Fabricated Using Variotherm Assisted Micro Injection Moulding. *Procedia CIRP* 71:390–395.
[201] Zhang SJ, Fang F-Z, Hu XT (2007) Advances of focused ion beam in micromachining technology. in Han S, Xing T, Li Y, Cui Z, (Eds.) *3rd International Symposium on Advanced Optical Manufacturing and Testing Technologies: Design, Manufacturing, and Testing of Micro- and Nano-Optical Devices and Systems*, SPIE, , 67240E.
[202] Zhang SJ, Fang F-Z, Xu ZW, Hu XT (2009) Controlled Morphology of Microtools Shaped Using Focused Ion Beam Milling Technique. *Journal of Vacuum Science & Technology B* 27(3):1304.
[203] Zhang X, Fang F-Z, Yu L, Jiang L, Guo Y (2013) Slow Slide Servo Turning of Compound Eye Lens. *Optical Engineering* 52(2):23401.
[204] Zhang X, Huang R, Liu K, Kumar AS, Shan X (2018) Rotating-Tool Diamond Turning of Fresnel Lenses on a Roller Mold for Manufacturing of Functional Optical Film. *Precision Engineering* 51:445–457.
[205] Zhang X, Jiang L, Zeng Z, Fang F-Z, Liu X (2015) High Angular Accuracy Manufacture Method of Micro V-Grooves Based on Tool Alignment by on-Machine Measurement. *Optics Express* 23(21):27819–27828.
[206] Zhang X, Li L, Li Z, Chan C, Zhu L, Lee W, Fang F-Z (2018) Highly Uniform Manufacturing Method for Large-Area Microlens Arrays. *International Journal of Advanced Manufacturing Technology* 95(1–4):99–108.
[207] Zhang X, Liu K, Shan X, Liu Y (2014) Roll-to-Roll Embossing of Optical Linear Fresnel Lens Polymer Film for Solar Concentration. *Optics Express* 22(Suppl 7): A1835–A1842.
[208] Zhang X, Liu K, Sunappan V, Shan X (2015) Diamond Micro Engraving of Gravure Roller Mould for Roll-to-Roll Printing of Fine Line Electronics. *Journal of Materials Processing Technology* 225:337–346.
[209] Zhang X, Zhu F, Sun G, Zhang H (2012) Fabrication and Characterization of Squama-Shape Micro/Nano Multi-Scale Silicon Material. *Science China Technological Sciences* 55(12):3395–3400.
[210] Zhou R, Cao J, Ehmann K, Xu C (2011) An Investigation on Deformation-Based Surface Texturing. *Journal of Manufacturing Science and Engineering* 133(6):61017.
[211] Zhou R, Cao J, Wang QJ, Meng F, Zimowski K, Xia ZC (2011) Effect of EDT Surface Texturing on Tribological Behavior of Aluminum Sheet. *Journal of Materials Processing Technology* 211(10):1643–1649.
[212] Zhou T, Yan J, Masuda J, Oowada T, Kuriyagawa T (2011) Investigation on Shape Transferability in Ultraprecision Glass Molding Press for Microgrooves. *Precision Engineering* 35(2):214–220.
[213] Zhu L, Li Z, Fang F-Z, Huang S, Zhang X (2018) Review on Fast Tool Servo Machining of Optical Freeform Surfaces. *International Journal of Advanced Manufacturing Technology* 95(5–8):2071–2092.
[214] Zhu W-L, Duan F, Zhang X, Zhu Z, Ju B-F (2018) A New Diamond Machining Approach for Extendable Fabrication of Micro-Freeform Lens Array. *International Journal of Machine Tools and Manufacture* 124:134–148.
[215] Zhu Z, To S, Ehmann KF, Xiao G, Zhu W (2016) A Novel Diamond Micro-/Nano-Machining Process for the Generation of Hierarchical Micro-/Nano-Structures. *Journal of Micromechanics and Microengineering* 26(3):35009.
[216] Zhu Z, To S, Zhang S (2015) Theoretical and Experimental Investigation on the Novel End-Fly-Cutting-Servo Diamond Machining of Hierarchical Micro-Nano-structures. *International Journal of Machine Tools and Manufacture* 94:15–25.
[217] Zou R, Yu Z, Li W, Guo M, Li J (2016) Influence of Porous Structure on the Machining Performance of Micro EDM. *Journal of Materials Processing Technology* 232:43–51.